Visualization of the Budding Yeast Cell Cycle

Jing Cui

Thesis submitted to the Faculty of the
Virginia Polytechnic Institute and State University
in partial fulfillment of the requirements for the degree of

Master of Science
in
Computer Science and Application

Yang Cao, Chair
Adrian Sandu
Shu-Ming Sun

July 31, 2017
Blacksburg, Virginia

Keywords: Visualization, Budding Yeast Cell Cycle, Deterministic Model, Hybrid Model, Mutants

Visualization of the Budding Yeast Cell Cycle

Jing Cui

ABSTRACT

The cell cycle of budding yeast is controlled by a complex chemically reacting network of a large group of species, including mRNAs and proteins. Many mathematical models have been proposed to unravel its molecular mechanism. However, it is hard for people with less training to visually interpret the dynamics from the simulation results of these models. In this thesis, we use the visualization toolkit D3 and jQuery to design a web-based interface and help users to visualize the cell cycle simulation results. It is essentially a website where the proliferation of the wild-type and mutant cells can be visualized as dynamical animation. With the help of this visualization tool, we can easily and intuitively see many key steps in the budding yeast cell cycle procedure, such as bud emergence, DNA synthesis, mitosis, cell division, and the current populations of species.

Visualization of the Budding Yeast Cell Cycle

Jing Cui

GENERAL AUDIENCE ABSTRACT

The cell cycle of budding yeast is controlled by a complex chemically reacting network. Many mathematical models have been proposed to unravel its molecular mechanism. However, it is hard to visually interpret the dynamics from the simulation results of these models. In this thesis, we use the visualization toolkit D3 and jQuery to design a web-based interface and help users to visualize the cell cycle simulation results. It is essentially a webpage where the proliferation of the wild-type and mutant cells can be visualized as dynamical animation.

Dedication

This thesis is dedicated to my parents.

For their constant support, encouragement and endless love

Acknowledgments

First of all, I would like to express my deepest appreciation to my advisor, Dr. Yang Cao, whose guidance assisted me throughout my research. I benefited much from his immense knowledge, wisdom, enthusiasm, humor, and kindness. I am also deeply grateful to Dr.John J.Tyson and Dr. Pavel Kraykivskiy for their valuable suggestions in the visualization of budding yeast cell cycle. I would like to thank my committee members, Dr. Adrian Sandu and Dr. Shu-Ming Sun for their insightful advice.

In addition, I wish to express my heartful thanks to my friends and labmates Shuo Wang, Mansooreh Ahmandian, Minghan Chen, and Tevien Toliver, who provided me a lot of assistance and enjoyable office life. Finally, I thank my family members for their love and encouragement.

Contents

List of Figures

List of Tables

Chapter 1

Overview

The cell cycle is a sequence of events during which a cell grows, replicates its DNA and proteins, and divides into two daughter cells that each contains the information and machinery necessary to start the process over again from the beginning [19, 20]. The whole process of cell cycle is very elaborate but robust, and it is regulated at various points known as checkpoints. At each checkpoint certain species, including genes, mRNAs and proteins, have to satisfy certain conditions for a specific event to occur. If those events occur when the corresponding checkpoints are not satisfied, the regulation fails and there may be serious and often fatal consequence. For example, the misregulation of cell cycle may cause serious diseases in human, including cancer. To better understand the cell proliferation mechanism in human, the budding yeast (Saccharomyces cerevisiae) cell cycle is considered an ideal model system, since the molecular machinery of DNA synthesis and mitosis is highly conserved among human and budding yeast cells, and it is quiet economically efficient in dealing with the budding yeast cells.

In general, budding yeast cells replicate DNA molecules in each chromosome precisely to form two identical sister chromatids that are held together by cohesins (tethering proteins) at the S phase (S for synthesis), and to partition their DNAs and proteins into two daughter cells at the M phase (M for mitosis and cytokinesis). S and M phases are separated by two gaps, called G_1 and G_2 phases (see Figure 1.1). So, usually, the stages of the cell cycle are $G_1 \to S \to G_2 \to M$. During the M phase, the replicated chromosomes are condensed and aligned by the mitotic spindles on the metaphase plane, then the sister chromatids are separated to opposite poles of the spindle, and finally, the cell divides such that each daughter cell has a complete set of chromosomes and roughly equal amount (about 42% vs. 58%) of proteins.

Molecular biologists have proposed different models (diagrams) of the regulatory network in the budding yeast cell cycle based on experimental observations on wild-type cells in glucose and galactose, as well as more than 200 mutant cases. Many mathematical models have been built to simulate the underlying mechanism in the molecular regulatory network.

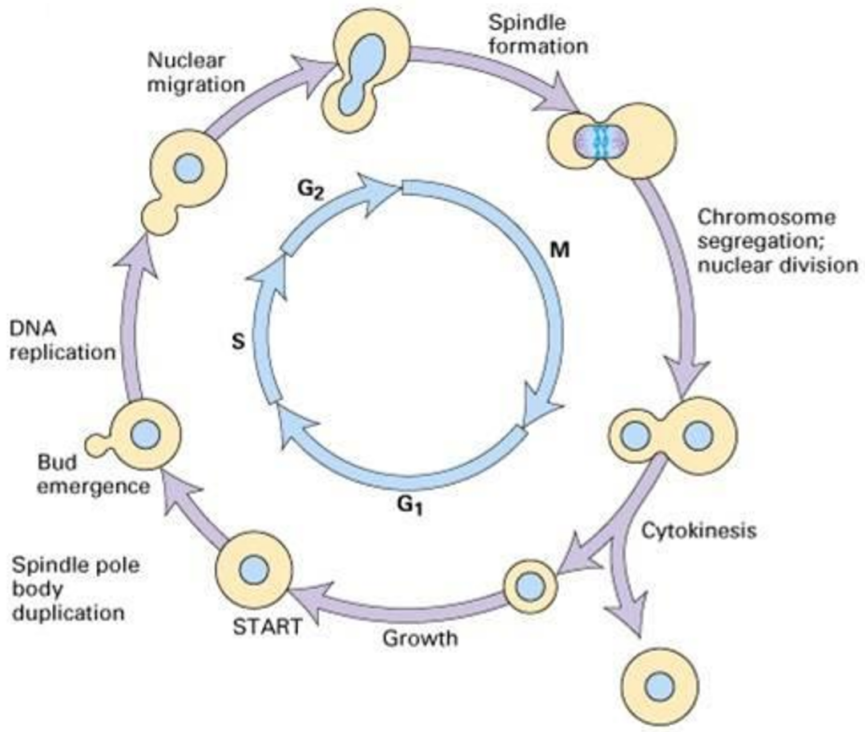

Figure 1.1: Budding yeast cell cycle.

Among them, one of the most important models is a deterministic model proposed by Chen et el. [7], which formulates the dynamics of all proteins by ordinary differential equations (ODEs). However, certain mutant cells are sensitive to noise, including molecular fluctuation (intrinsic noise) and uneven division (extrinsic noise). In budding yeast cells, the intrinsic noise comes primarily from fluctuations of mRNA populations. In order to better represent the intrinsic noise, about 19 mRNAs and their corresponding synthesis and degradations are added to Chen's model in a recent work by Wang et el. [37] .

Although deterministic models can successfully capture the average behavior of cells, they fail to simulate the variability caused by noise. In order to model partially viable mutant cells, the Gillespie's stochastic simulation algorithm (SSA) is a suitable method to convert the deterministic model into its stochastic equivalent. However, SSA is not efficient for the budding yeast cell whose molecular mechanism is complex and controlled by more than 42 types of proteins, some with large populations.

Wang et el. [37] applied the hybrid method first introduced in Liu et al. [17], which incorporated the methods of the SSA and ODEs, to simulate the budding yeast cell cycle. The hybrid model in [37] simulates the synthesis and degradation of 19 selected mRNAs by SSA, while conserving the protein interactions from Chen's model. The populations of mRNAs are small and their fluctuations are the primary source of the intrinsic noise. So the hybrid model can improve the accuracy and maintain a similar efficiency of the deterministic

model.

In order to observe the cell cycle procedure of the budding yeast, we want to know whether the mutant is viable or inviable (i.e. fail to proliferate), as well as the populations of species for each event. If it is viable, what is the mass of the cell at each checkpoint of the cell cycle? What is the duration of each phase? If it is inviable, at what phase does the cell stop the cell cycle dynamics? All these features are hard to see intuitively from raw numerical results of the mathematical models, which are collections of data. Even with help of plotting tools, it is hard for people without long time training to directly link the model simulation results with the phenotypes of budding yeast cells.

One of the solutions to this problem is the data visualization. Chen et el. [7] used the line chart (Figure 4.1) to simulate the cell size, and concentrations of proteins so that the estimation of the model can be investigated. However, it requires a solid background of the control mechanism of the budding yeast cell cycle to read the line chart and obtain useful information from it. This violates one principle of effectively visualization that representing complicated information in a way that can be quickly and easily understood by specialists and non- specialists alike. In addition, the overall graph of the cell cycle is not visible from the line chart, and so observers have to pay time and cognitive effort to form a mental model of the cell cycle. Moreover, every adjustment of time range (time axis) and species (values on the y axis) is implemented by changing the code.

We build a powerful web-based interface, with simple menus and several selection buttons, to guide users to create a visualization of the simulation results. It is essentially a web page where users can choose the mutant type, the model simulated, the simulation time, proteins to be displayed, and so on, to visualize the behavior of the budding yeast cell cycle mechanism. The created visualization is a combination of interactive multi-line chart (Figure 4.4) and animated graphics of the cell (Figure 4.5). The interactive multi-line chart inherits all of the functions and advantages of static line chart in [7] and allow users to control its displayed species and time line and hover on it to see the accurate values of each specie. Users can play or drag the time slider to view the animation of the budding yeast cell cycle illustrating the simulated graph of the cell at each moment.

The outline of this thesis is as follows. Chapter 2 illustrates the regulation of a general cell cycle procedure. The molecular mechanism of the regulatory network in the budding yeast cell cycle are described. All the checkpoints that ensure the proper division of the cell and the corresponding reactions or proteins described in Chapter 2 are the basis of the mathematical models of Chapter 3. In Chapter 3, we introduce three mathematical models of the budding yeast cell cycle in detail, including Chen's deterministic model, Chen's model with mRNAs added, and Wang's hybrid model. The detailed design of the visualization for all of the three mathematical models is explained in Chapter 4. Then, some special mutants are chosen to test the visualization and to compare the results of mathematical models with observed phenotypes of the cells in Chapter 5. At the end, Chapter 6 gives a conclusion of our work and some suggestions to improve the visualization in the future.

Chapter 2

Regulation of Cell Cycle

2.1 Introduction

The cell cycle consists of a sequence of events during which a cell grows, replicates its genetic material (DNAs, chromosomes, mRNAs and proteins), and divides into two daughter cells that each contains the information and machinery necessary to start the process over again from the beginning. Scientists have identified four characteristic stages of the cell cycle: $G_1 \rightarrow S \rightarrow G_2 \rightarrow M$. The $G1$, S and G_2 phases, collectively called interphase, occupy a much longer part of the cell than the M phase. For a cell cycle of rapidly dividing human cells that lasts about 24 hours, the M phase only lasts about 30 minutes [20]. During the interphase the individual chromosome is distributed within the nucleus and cannot be distinguished. G_1 and G_2 are two gaps that separate S and M phases. They provide time for the cell to grow and to prepare suitable environment for DNA synthesis and mitosis. DNA replication occurs in the S phase (S denotes for synthesis), and the two daughter chromosomes, which remain attached to each other, are called sister chromatids. In the M phase (M denotes for mitosis and cytokinesis) sister chromatids are pulled apart by the mitotic spindle, and cytoplasm divides to form two daughter cells. Mitosis consists of prophase, metaphase, anaphase, and telophase. Briefly, chromosomes condense and become visibly distinct from each other in the prophase; two members of each pair of sister chromatids attach to spindle fibers, long fibers that radiate throughout the cell from opposite spindle poles, and move to a midway between the two spindle poles until all the chromosomes are lined up during the metaphase; sister chromatids separate from one another and move to the opposite poles along the spindles is the beginning of the anaphase; as the chromosomes move near the poles, the cell splits itself into two daughter cells in the telophase. During the final stage, called cytokinesis, the cell is completely divided. Figure 2.1 illustrates the stages of the cell cycle.

Despite certain features of the cell cycle process vary greatly from one cell type to another,

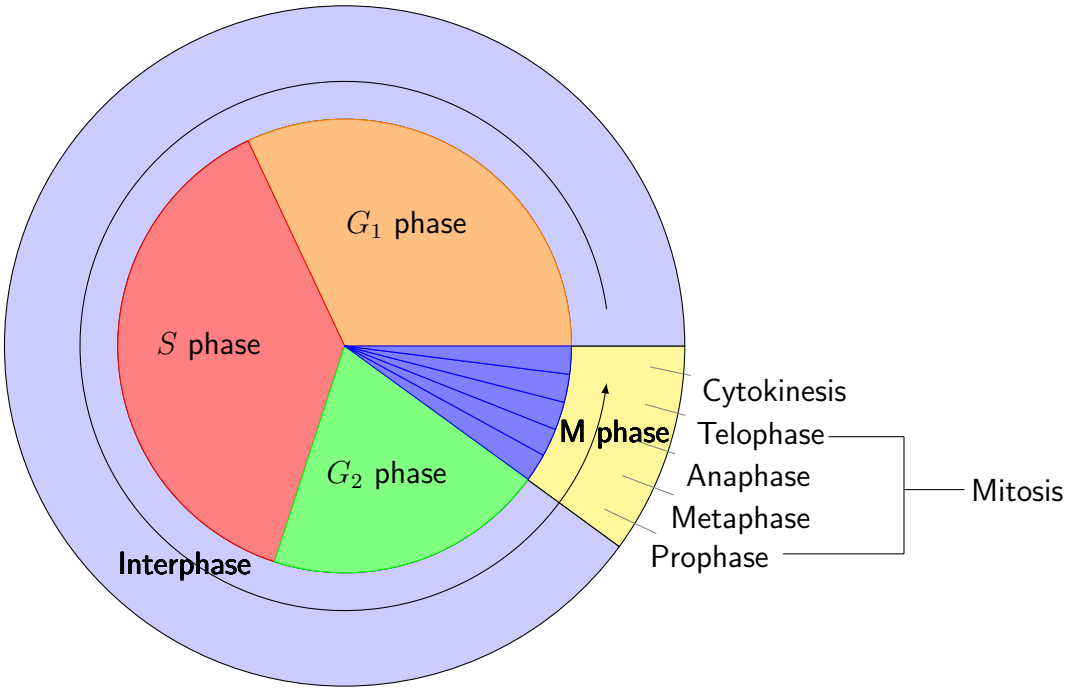

Figure 2.1: Stages of the cell cycle.

the basic organization of the cycle and its control system are essentially the same in all eukaryotic cells. Animals, plants, fungi (such as yeasts, mushroom) and protists (such as algae, plankton) are all eukaryotes. Human cells are also categorically eukaryotic organisms. Scientists have found that the unicellular budding yeast (Saccharomyces cerevisiae) cells have similar mechanisms of cell-cycle control to human cells. It is much faster and cheaper to cultivate budding yeast cells than to cultivate human cells in laboratories. So the budding yeast cell cycle system can be used as a model system to study the cell cycle, in order to understand the cell cycle control mechanisms of human cells.

2.2 Budding Yeast Cell Cycle

A budding yeast cell divides by forming a bud, which first appears during its G_1 phase and grows steadily until it separates from the mother cell after mitosis. Unlike most multicellular organisms, whose cell nucleus envelope breaks down and then re-forms during mitosis (open mitosis), the nucleus of a budding yeast cell stays intact throughout mitosis (closed mitosis) (Figure 1.1).

A specific type of cell cycle control mechanisms, known as cell cycle checkpoints, can ensure the proper division of the cell. The G_1 checkpoint and the spindle assembly checkpoint are two major checkpoints of the budding yeast cell cycle process. They are enforced by a

family of protein kinases known as Cdk/cyclin complexes. Budding yeast has only one Cdk (called Cdc28) and nine different cyclins (Cln1-3, Clb1-6). Depending on different cyclin partner that binds to Cdc28, Cdc28/cyclin dimers may accomplish different specific tasks and control the progression of cell cycle events. The activations of these Cdc28/cyclin dimers are influenced by several proteins (Mcm1, Sic1, Cdc20, etc.) that drive the synthesis and degradation of corresponding Cdk and cyclins.

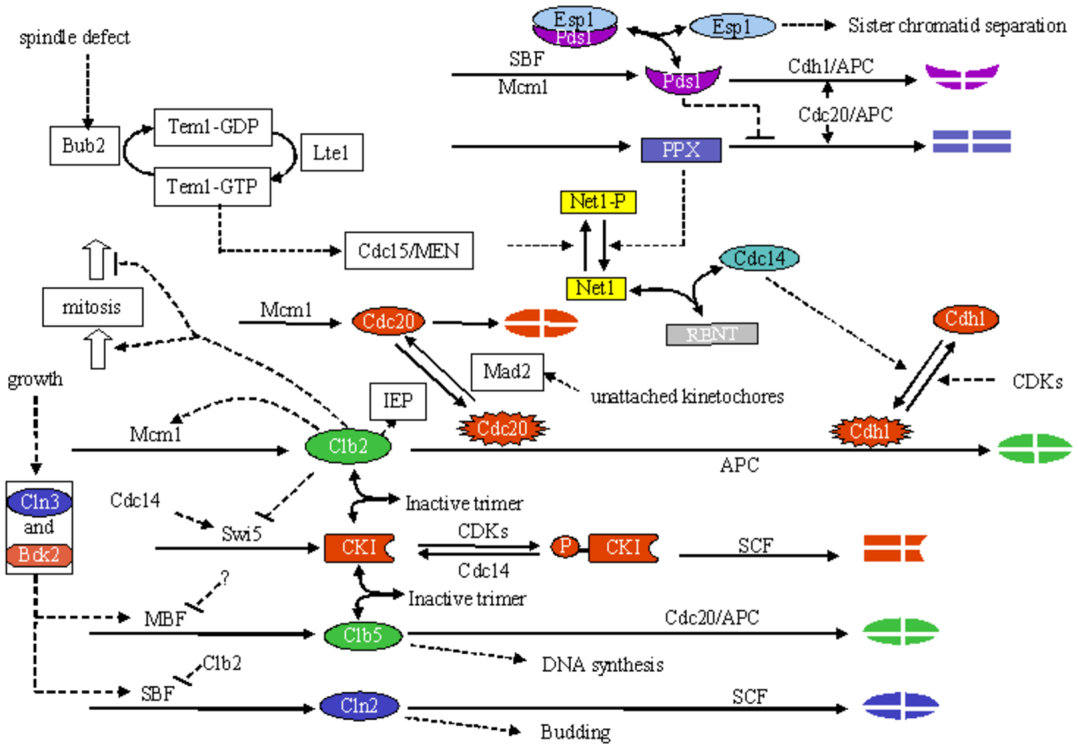

Figure 2.2: Consensus model of the regulatory network in the budding yeast.

Molecular biologists have proposed a hypothetical molecular mechanism that regulates DNA synthesis, bud emergence, mitosis, and cell division in the budding yeast, which is described in Figure 2.2 [7]. In this diagram (Figure 2.2), Cln2 stands for both Cln1 and Cln2, Clb5 stands for both Clb5 and Clb6, and Clb2 stands for both Clb1 and Clb2. Cdc28 is not shown explicitly, because it is abundant and it combines with cyclins rapidly. We read the diagram from the bottom-left corner towards the top-right corner. Biochemical reactions are represented by solid arrows. Dashed lines indicate how components may influence one another. For the full explanation of this diagram, please check the web site at `http://mpf.biol.vt.edu`. Here, we only introduce some important proteins that will be displayed in our visualization of the budding yeast cell cycle.

- Cln3: One of cell cycle cyclins. The Cdc28/Cln3 complex initiates the Start event.

Cln3 protein and mRNA levels are relatively constant in the budding yeast cell cycle [34, 40].

- Cln2: One of cell cycle cyclins. In the model, Cln2 actually represents both Cln1 and Cln2. In the cell cycle regulation mechanism, Cdc28/Cln2 induces bud emergence. Cln2 protein and mRNA levels fluctuate in a cell cycle, and reach the highest values in late G1 phase [29, 34]. Cln2 deletion mutant shows delay in budding [9, 30].

- Clb2 (represents both Clb1 and Clb2): The Cdc28/Clb2 complex is essential for the mitosis process. Clb2 protein and mRNA levels fluctuate in a cell cycle, and reach the highest values in the M phase [27, 29].

  The activity of Clb2 is high about 10 minutes before the anaphase [31], and has to be inhibited for cell to exit from mitosis [32, 45]. Clb2 stimulates the synthesis of Cdc20 [23]. Clb2 deletion mutant shows arrest in the G2 phase [31]. The Clb2 half-life is very short (<1 minute) in cells arrested in the G1 phase, but long (>2 hours) in S or M phase arrested cells [2, 13].

- Clb5 (represents both Clb5 and Clb6): The Cdc28/Clb5 complex is responsible for the initiation of DNA synthesis in the S phase; Clb5 deletion mutant shows delay in DNA replication [24]. Clb5 protein and mRNA levels fluctuate in a cell cycle, and reach the highest values in late G1 phase [24, 29]. Clb5 phosphorylates Cdh1 and Cdc6 [10, 44].

- Cdh1: Cdh1 is necessary for the degradation of Clb2 during the telophase [5, 43]. Cdh1 protein and mRNA levels fluctuate slightly in the budding yeast cell cycle [15, 44].

- Cdc14: Cdc14 is needed for exit of mitosis [4, 36]. Cdc14 protein and mRNA levels are relatively constant in the budding yeast cell cycle [29].

- Cdc20: Cdc20 is also needed for exit of mitosis, required in partial degradation of Clb2 at the anaphase [5, 38, 43], Clb5 degradation [14, 28], and Pds1 proteolysis. Cdc20 deletion mutant shows arrest in the M phase, with high Clb2 activity and unseparated sister chromatids [1, 16]. Cdc20 protein and mRNA levels fluctuate in a cell cycle, whose patterns similar to that of Clb2 [23, 27].

- Esp1: Esp1 is partly bound to the spindles during the metaphase-anaphase transition [8], needed for sister chromatids separation at the anaphase [21, 42]. The activity of Esp1 is inhibited when Pds1 bands to it [8]. To ensure the separation of sister chromatids, Pds1 degradation happens at anaphase which requires Cdc20 [41]. Esp1 transcription is constant during the budding yeast cell cycle [29]. But Pds1 protein and transcription fluctuate, Esp1 protein peaks at the M phase and its transcription peaks at the G1 or S phase [29, 33].

- Sic1 and Cdc6: Both of them are inhibitors of Cdk kinases, Sic1 inhibits Cdc28/Clb2 and Cdc28/Clb5, and Cdc6 inhibits Cdc28/Clb2.

Chapter 3

Modeling the Budding Yeast Cell Cycle Control Mechanism

3.1 Introduction

Figure 2.2 summarizes the interactions of many important components of the budding yeast cell cycle. It is a complex biochemical network and is hard to be comprehended intuitively. Many questions can be raised upon a mathematical model of the budding yeast cell cycle. For example, how good is a specific hypothesis? Can it account for the growth and division of the intact cell? The classical approach to answer these questions is to convert the mechanism in Figure 2.2 into a mathematical model and investigate the properties of it.

Several deterministic models have been proposed, in which the control mechanisms are formulated as a set of ordinary differential equations(ODEs). In this thesis, we will focus on one of the most successful models in literature, which was originally proposed by Chen et al. [6] and then improved in [7]. So far, the numerical results of Chen's model are in great agreement with physiological properties of 120 mutant strains out of 131 studied mutant cases in the budding yeast.

In the last two decades, more and more scientists have paid attention to noise in cellular systems. During a cell cycle, there exists intrinsic noise from fluctuations of molecule numbers present within a single cell and extrinsic noise from uneven division. Especially, the cells with mutations are more sensitive to noise than wild type cells. Although Chen's model successfully unravels the dynamics property of wild type cells and correctly predicts the behavior of different types of mutant cells, it does not include noise in the model. section 3.3 presents an improved Chen's model, which includes intrinsic noise with detailed mRNA dynamics.

In order to enhance the accuracy of the model, it is necessary to convert the deterministic

model to its stochastic equivalent and simulate it through the Gillespie's stochastic simulation algorithm (SSA). However, the low efficiency is a bottleneck of SSA. In section 3.3, we also present a hybrid (ODE/SSA: a combination of ODEs and SSA) stochastic model, which reduces the computational cost while still accurately modeling the effects of noise [37].

3.2 Chen's Model

Molecular biologists have proposed different models (diagrams) of the regulatory network in the budding yeast cell cycle based on experimental observations on wild-type cells in glucose and galactose, as well as more than 200 mutant cases. A hypothetical molecular mechanism in Figure 2.2 summarizing the principal chemical reactions of genes and proteins that control the budding yeast cell cycle as a set of components interconnected by reactions (arrows). By applying general principles of biochemical kinetics, Chen et al. converted the mechanism in Figure 2.2 into a set of ODEs that determinate how the system dynamics will change during time. In Chen's model, the concentrations of all species are represented as time-varying variables, called the state of the system. The next state can be determined from the current state and chemical reactions in the model. These chemical reactions can model biological events such as synthesis, degradation, activation, inhibition, binding, and release of those species. Each reaction proceeds at a rate determined by the current state of the system and kinetic parameters of the reaction. It is important to realize that there is no unique correspondence between a wiring diagram and a set of mathematical equations; the same mechanism can be represented by different forms of equations. For example, some components can be described by differential equations and others by algebraic equations, and moreover, most kinetic parameters have to be estimated based on limited experimental data.

All the ODEs and corresponding reaction rates and kinetic constants can be found in Chen et al., 2004 [7] and its companion website: `http://mpf.biol.vt.edu`. The model was transferred to a Matlab version and its code can be also downloaded from the companion website. In order to test the model or wiring diagram (Figure 2.2), Chen et al. compared the computed results with the experimental behaviors for 2 wild-types and 131 mutants (Table 3.1). For each mutant, only the parameters that are governed by the nature of the mutation need to be changed in the deterministic model. There are total 11 mutants that the model doesn't agree with observations. They are No. 34, 36, 40, 41, 45, 48, 51, 52, 53, 80, 119 in Table 3.1. We will also compare the numerical solution of those cases in Table 3.1 to the experimental results through our designed visualization in Chapter 5, which will give more intuitive results.

Table 3.1: Tested 2 wild-types and 131 mutants.

Mutant Type	**No.**	**Mutant**
Wild-types	1	WT in glucose
	2	WT in galactcose

Table 3.1: (Continued)

Cln mutants	3	$cln1\Delta$ $cln2\Delta$
	4	$GAL\text{-}CLN2$ $cln1\Delta$ $cln2\Delta$
	5	$cln1$ Δ $cln2\Delta$ $sic1\Delta$
	6	$cln1\Delta cln2\Delta cdh1\Delta$
	7	$GAL\text{-}CLN2$ $cln1\Delta$ $cln2\Delta$ $cdh1\Delta$
	8	$cln3\Delta$
	9	$GAL\text{-}CLN3$
Bck2 mutants	10	$bck2\Delta$
	11	Multi-copy $BCK2$
	12	$cln1\Delta$ $cln2\Delta$ $bck2\Delta$
	13	$cln3\Delta$ $bck2\Delta$
	14	$cln3\Delta$ $bck2\Delta$ $GAL\text{-}CLN2$ $cln1\Delta$ $cln2\Delta$
	15	$cln3\Delta$ $bck2\Delta$ multi-copy $CLN2$
	16	$cln3\Delta$ $bck2\Delta$ $sic1\Delta$
cln1 cln2 cln3 strain	17	$cln1\Delta$ $cln2\Delta$ $cln3\Delta$
	18	$cln1\Delta$ $cln2\Delta$ $cln3\Delta$ $GAL\text{-}CLN2$
	19	$cln1\Delta$ $cln2\Delta$ $cln3\Delta$ $GAL\text{-}CLN3$
	20	$cln1\Delta$ $cln2\Delta$ $cln3\Delta$ $sic1\Delta$
	21	$cln1\Delta$ $cln2\Delta$ $cln3\Delta$ $cdh1\Delta$
	22	$cln1\Delta$ $cln2\Delta$ $cln3\Delta$ multi-copy $CLB5$
	23	$cln1\Delta$ $cln2\Delta$ $cln3\Delta$ $GAL\text{-}CLB5$
	24	$cln1\Delta$ $cln2\Delta$ $cln3\Delta$ multi-copy $BCK2$
	25	$cln1\Delta$ $cln2\Delta$ $cln3\Delta$ $GAL\text{-}CLB2$
	26	$cln1\Delta$ $cln2\Delta$ $cln3\Delta$ apc^{ts}
Cdh1, Sic1 and Cdc6 mutants	27	$sic1\Delta$
	28	$GAL - SIC1$
	29	$GAL - SIC1 - db\Delta$
	30	$GAL - SIC1 cln1\Delta cln2\Delta$
	31	$GAL - SIC1 GAL - CLN2 cln1\Delta cln2\Delta$
	32	$GAL - SIC1 cln1\Delta cln2\Delta cdh1\Delta$
	33	$GAL - SIC1 GAL - CLN2 cln1\Delta cln2\Delta cdh1\Delta$
	34	$cdh1\Delta$
	35	$Cdh1$ constitutively active
	36	$sic1\Delta$ $cdh1\Delta$
	37	$sic1\Delta$ $cdh1\Delta$ $GALL\text{-}CDC20$
	38	$cdc6\Delta 2\text{-}49$
	39	$sic1\Delta$ $cdc6\Delta 2\text{-}49$
	40	$cdh1\Delta$ $cdc6\Delta 2\text{-}49$
	41	$sic1\Delta$ $cdc6\Delta 2\text{-}49$ $cdh1\Delta$
	42	$sic1\Delta$ $cdc6\Delta 2\text{-}49$ $cdh1\Delta$ $GALL\text{-}CDC20$
	43	$swi5\Delta$
	44	$swi5\Delta$ $GAL\text{-}CLB2$
	45	$swi5\Delta$ $cdh1\Delta$
	46	$swi5\Delta$ $cdh1\Delta$ $GAL\text{-}SIC1$
Clb1 Clb2 mutants	47	$clb1\Delta$ $clb2\Delta$
	48	$CLB1$ $clb2\Delta$
	49	$GAL\text{-}CLB2$
	50	Multi-copy $GAL\text{-}CLB2$
	51	$CLB1$ $clb2\Delta$ $cdh1\Delta$
	52	$CLB1$ $clb2\Delta$ $pds1\Delta$
	53	$GAL\text{-}CLB2$ $sic1\Delta$
	54	$GAL\text{-}CLB2$ $cdh1\Delta$
	55	$CLB2\text{-}db\Delta$
	56	$CLB2\text{-}db\Delta$ in galactose
	57	$CLB2\text{-}db\Delta$ multicopy $SIC1$
	58	$CLB2\text{-}db\Delta$ $GAL - SIC1$
	59	$CLB2\text{-}db\Delta$ multi-copy $CDC6$
	60	$CLB2\text{-}db\Delta$ $clb5\Delta$
	61	$CLB2\text{-}db\Delta$ $clb5\Delta$ in galactose
	62	$GAL\text{-}CLB2\text{-}db\Delta$
Clb5 Clb6 mutants	63	$clb5\Delta$ $clb6\Delta$
	64	$cln1\Delta$ $cln2\Delta$ $clb5\Delta$ $clb6\Delta$
	65	$GAL\text{-}CLB5$
	66	$GAL\text{-}CLB5$ $sic1\Delta$
	67	$GAL\text{-}CLB5$ $cdh1\Delta$
	68	$CLB5\text{-}db\Delta$
	69	$CLB5\text{-}db\Delta$ $sic1\Delta$
	70	$CLB5\text{-}db\Delta$ $pds1\Delta$
	71	$CLB5\text{-}db\Delta$ $pds1\Delta$ $cdc20\Delta$
	72	$GAL\text{-}CLB5\text{-}db\Delta$

Table 3.1: (Continued)

Cdc20 mutants	73	$cdc20^{ts}$
	74	$cdc20\Delta$ $clb5\Delta$
	75	$cdc20\Delta$ $pds1\Delta$
	76	$cdc20\Delta$ $pds1\Delta$ $clb5\Delta$
	77	$GAL\text{-}CDC20$
	78	$cdc20^{ts}$ $mad2\Delta$
	79	$cdc20^{ts}bub2\Delta$
Pds1/Esp1 interaction	80	$pds1\Delta$
	81	$esp1^{ts}$
	82	$PDS1\text{-}db\Delta$
	83	$GAL\text{-}PDS1\text{-}db\Delta$
	84	$GAL\text{-}PDS1\text{-}db\Delta$ $esp1^{ts}$
	85	$GAL\text{-}ESP1cdc20^{ts}$
Men pathway mutants	86	$tem1\Delta$
	87	$GAL\text{-}TEM1$
	88	$Tem1^{ts}$ Multi-copy $CDC15$
	89	$tem1^{ts}GAL\text{-}CDC15$
	90	$tem1\Delta$ $net1^{ts}$
	91	$tem1\Delta$ multi-copy $CDC14$
	92	$cdc15\Delta$
	93	Multi-copy $CDC15$
	94	$cdc15^{ts}$ multi-copy $TEM1$
	95	$cdc15\Delta net1^{ts}$
	96	$cdc15^{ts}$ multi-copy $CDC14$
Exit-of-mitosis mutants	97	$net1^{ts}$
	98	$GAL\text{-}NET1$
	99	$cdc14^{ts}$
	100	$GAL\text{-}CDC14$
	101	$GAL\text{-}NET1$ $GAL\text{-}CDC14$
	102	$net1\Delta cdc20-ts$
	103	$cdc14^{ts}$ $GAL\text{-}SIC1$
	104	$cdc14^{ts}$ then $GAL\text{-}SIC1$
	105	$cdc14^{ts}$ $sic1\Delta$
	106	$cdc14^{ts}$ $cdh1\Delta$
	107	$cdc14^{ts}$ $GAL\text{-}CLN2$
	108	$TAB6\text{-}1$
	109	$TAB6\text{-}1$ $cdc15\Delta$
	110	$TAB6\text{-}1$ $clb5\Delta$ $clb6\Delta$
	111	$TAB6\text{-}1$ $CLB1$ $clb2\Delta$
Cdh1, Sic1 and Cdc6 mutants	112	$mad2\Delta$
	113	$bub2\Delta$
	114	$mad2\Delta$ $bub2\Delta$
	115	WTI in nocodazole
	116	$mad2\Delta$ in nocodazole
	117	$mad2\Delta$ $Gal\text{-}Tem1$ in nocodazole
	118	$mad2\Delta$ $pds1\Delta$ in nocodazole
	119	$bud2\Delta$ in nocodazole
	120	$bud2\Delta$ $pds1\Delta$ in nocodazole
	121	$bud2\Delta$ $mad2\Delta$ in nocodazole
	122	$pds1\Delta$ in nocodazole
	123	$net1^{ts}$ in nocodazole
APC mutants	124	$APC\text{-}A$
	125	$APC\text{-}Acdh1\Delta$
	126	$APC\text{-}Acdh1\Delta$ in galactose
	127	$APC\text{-}Acdh1\Delta$ multi-copy $SIC1$
	128	$APC\text{-}Acdh1\Delta GAL\text{-}SIC1$
	129	$APC\text{-}Acdh1\Delta$ multi-copy $CDC6$
	130	$APC\text{-}Acdh1\Delta GAL\text{-}CDC6$
	131	$APC\text{-}Acdh1\Delta$ multi-copy $CDC20$
	132	$APC\text{-}Asic1\Delta$
	133	$APC\text{-}AGAL\text{-}CLB2$

3.3 Chen's Model with mRNA

The fluctuations of species populations, which cause intrinsic noise, can be measured by the coefficient of variation (CV). Pedraza and Paulsson [22] derived that, for a protein involved in simple synthesis and degradation process, its CV can be formulated as

$$CV = \sqrt{\frac{1}{N_p} + \frac{\tau_m}{\tau_m + \tau_p}\frac{1}{N_m}},$$

where N_p and N_m are the average populations of the protein and its mRNA, τ_p and τ_m are their corresponding half-life times, respectively. Normally $N_m < 10$, but N_p is around hundreds or thousands even in a cell of small volume. So $N_p << N_m$. We also have $\tau_p \leq \tau_m$ in many cases. Thus the CV can also be approximated by

$$CV \approx \sqrt{\frac{1}{2N_m}},$$

which implies that the intrinsic noise is primarily generated by mRNAs populations.

Table 3.2: Added mRNAs.

Unregulated mRNAs	**Regulated mRNAs**
mCdh1	mCln2
mTem1	mClb5
mCdc15	mClb2
mCdc14	mSic1
mNet1	mCdc6
mPPx	mSwi5
mEps1	mCdc20
mSBF	mPds1
mMBF	
mMcm1	
mAPC	

The mRNA whose synthesis is regulated by proteins is called regulated mRNA, otherwise, is called unregulated mRNA. In order to improve Chen's model, the synthesis and degradation of 11 unregulated mRNAs and 8 regulated mRNAs (Table 3.2) are added. The reactions associated with mRNAs are simple (Figure 3.1), which can be formulated as a linear chain reaction model,

$$\varnothing \xrightarrow{k_{ms}} mRNA \xrightarrow{k_{md}} \varnothing,$$

where the degradation rate $k_{md} = \frac{ln(2)}{\text{half-life time of the mRNA}}$, the synthesis rate $k_{ms} = k_{md} \cdot \langle mRNA \rangle$ for an unregulated mRNA, $\langle mRNA \rangle$ represents the mean molecule number of

mRNA, and $k_{ms} = k_{md}\,(\sum_{i=1}^{n} k_{ms,i} \cdot p_i)$ for a regulated mRNA, p_i is the protein molecule number [37].

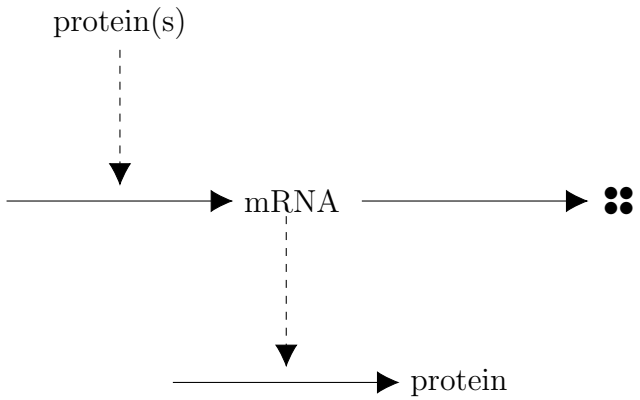

Figure 3.1: Reactions associated with mRNAs.

3.4 Hybrid Model

Although Chen's Model with mRNA (in section 3.3) does include noise, this deterministic model can only capture the average behavior of the budding yeast cells. The fluctuations of molecules in living cells and the perturbations of environment are discrete and stochastic rather than continuous and deterministic. So the effective method to model the control mechanism with noise is to convert the deterministic model to its stochastic equivalent. One widely used method for stochastic simulation is Gillespie's stochastic simulation algorithm (SSA) [11, 12]. However, the time complexity of SSA increases proportionally with the number of reactions. In order to improve the efficiency, Wang et al. [37] presented a hybrid (ODE/SSA) stochastic model of the budding yeast cell cycle. It simulates the synthesis and degradation of 19 mRNAs (introduced in section 3.3), whose reactants have low populations by slow SSA, while it derives the interactions of 42 proteins directly from Chen's model (in section 3.1).

In Chen's model, proteins are represented in concentrations. While, SSA models species with discrete numbers of molecules. In order to establish the hybrid model, the first step is to convert each state variable in Chen's model from concentration to its corresponding population. The approach is discussed by Ball et al. [3] in detail. Meanwhile, reaction rates and some constants need to be scaled correspondingly so that the dynamics of the transformed system of ODEs are equivalent to the original model. Then, the terms related to protein synthesis are replaced by the terms in the form of $k_t * mRNA$ to make sure the hybrid model is consistent with the translation processes from mRNAs to proteins, where k_t is a rate constant for translation of the protein from its specific mRNA molecule [37]. One reason is that the synthesis of each type of protein in the hybrid model is determined by

the population of mRNA. The ODEs used to simulated the mass and proteins are listed in Table 3.3.

Table 3.3: ODEs related to mass and proteins in Hybrid model.

$$\frac{\text{d mass}}{\text{dt}} = k_g \cdot \text{mass}$$

$$\frac{\text{d Cln2}}{\text{dt}} = k_{s,n2} \cdot \text{mCln2} \cdot \text{mass} - k_{d,n2} \cdot \text{Cln2} + k_g \cdot \text{Cln2}$$

$$\frac{\text{d Clb5}}{\text{dt}} = k_{s,b5} \cdot \text{mClb5} \cdot \text{mass} + (k_{d3,c1} \cdot \text{C5P} + k_{di,b5} \cdot \text{C5}) + (k_{d3,f6} \cdot \text{F5P} + k_{di,f5} \cdot \text{F5}) - (V_{d,b5} + k_{as,b5} \cdot \frac{\text{Sic1}}{\text{mass}} + k_{as,f5} \cdot \frac{\text{Cdc6}}{\text{mass}}) \cdot \text{Clb5} + k_g \cdot \text{Clb5}$$

$$\frac{\text{d Clb2}}{\text{dt}} = k_{s,b2} \cdot \text{mClb2} \cdot \text{mass} + (k_{d3,c1} \cdot \text{C2P} + k_{di,b2} \cdot \text{C2}) + (k_{d3,f6} \cdot \text{F2P} + k_{di,f2} \cdot \text{F2}) - (V_{d,b2} + k_{as,b2} \cdot \frac{\text{Sic1}}{\text{mass}} + k_{as,f2} \cdot \frac{\text{Cdc6}}{\text{mass}}) \cdot \text{Clb2} + k_g \cdot \text{Clb2}$$

$$\frac{\text{d Sic1}}{\text{dt}} = k_{s,s1} \cdot \text{mSic1} + (V_{d,b2} + k_{di,b2}) \cdot \text{C2} + (V_{d,b5} + k_{di,b5}) \cdot \text{C5} + k_{pp,c1} \cdot \frac{\text{Cdc14} \cdot \text{Sic1P}}{\text{mass}} - (k_{as,b2} \cdot \frac{\text{Clb2}}{\text{mass}} + k_{as,b5} \cdot \frac{\text{Clb5}}{\text{mass}} + V_{kp,c1}) \cdot \text{Sic1} + k_g \cdot \text{Sic1}$$

$$\frac{\text{d Sic1P}}{\text{dt}} = V_{kp,c1} \cdot \text{Sic1} - (k_{pp,c1} \cdot \frac{\text{Cdc14}}{\text{mass}} + k_{d3,c1}) \cdot \text{Sic1P} + V_{d,b2} \cdot \text{C2P} + V_{d,b5} \cdot \text{C5P} + k_g \cdot \text{Sic1P}$$

$$\frac{\text{d C2}}{\text{dt}} = k_{as,b2} \cdot \frac{\text{Clb2} \cdot \text{Sic1}}{\text{mass}} + k_{pp,c1} \cdot \frac{\text{Cdc14} \cdot \text{C2P}}{\text{mass}} - (k_{di,b2} + V_{d,b2} + V_{kp,c1}) \cdot \text{C2} + k_g \cdot \text{C2}$$

$$\frac{\text{d C5}}{\text{dt}} = k_{as,b5} \cdot \frac{\text{Clb5} \cdot \text{Sic1}}{\text{mass}} + k_{pp,c1} \cdot \frac{\text{Cdc14} \cdot \text{C5P}}{\text{mass}} - (k_{di,b5} + V_{d,b5} + V_{kp,c1}) \cdot \text{C5} + k_g \cdot \text{C5}$$

$$\frac{\text{d C2P}}{\text{dt}} = V_{kp,c1} \cdot \text{C2} - (k_{pp,c1} \cdot \frac{\text{Cdc14}}{\text{mass}} + k_{d3,c1} + V_{d,b2}) \cdot \text{C2P} + k_g \cdot \text{C2P}$$

$$\frac{\text{d C5P}}{\text{dt}} = V_{kp,c1} \cdot \text{C5} - (k_{pp,c1} \cdot \frac{\text{Cdc14}}{\text{mass}} + k_{d3,c1} + V_{d,b5}) \cdot \text{C5P} + k_g \cdot \text{C5P}$$

$$\frac{\text{d Cdc55}}{\text{dt}} = k_{s,ppx} \cdot \text{mass} \cdot \text{mCdc55} - V_{d,ppx} \cdot \text{Cdc55} + k_g \cdot \text{Cdc55}$$

$$\frac{\text{d Cdc6P}}{\text{dt}} = V_{kp,f6} \cdot \text{Cdc6} - (k_{pp,f6} \cdot \frac{\text{Cdc14}}{\text{mass}} + k_{d3,f6}) \cdot \text{Cdc6P} + V_{d,b2} \cdot \text{F2P} + V_{d,b5} \cdot \text{F5P} + k_g \cdot \text{Cdc6P}$$

$$\frac{\text{d Cdc6}}{\text{dt}} = k_{s,c6} \cdot \text{mCdc6} + (V_{d,b2} + k_{di,f2}) \cdot \text{F2} + (V_{d,b5} + k_{di,f5}) \cdot \text{F5} + k_{pp,f6} \cdot \frac{\text{Cdc14} \cdot \text{Cdc6P}}{\text{mass}} - (k_{as,f2} \cdot \frac{\text{Clb2}}{\text{mass}} + k_{as,f5} \cdot \frac{\text{Clb5}}{\text{mass}} + V_{kp,f6}) \cdot \text{Cdc6} + k_g \cdot \text{Cdc6}$$

$$\frac{\text{d F2}}{\text{dt}} = k_{as,f2} \cdot \text{Clb2} \cdot \frac{\text{Cdc6}}{\text{mass}} + k_{pp,f6} \cdot \frac{\text{Cdc14} \cdot \text{F2P}}{\text{mass}} - (k_{di,f2} + V_{d,b2} + V_{kp,f6}) \cdot \text{F2} + k_g \cdot \text{F2}$$

$$\frac{\text{d F5}}{\text{dt}} = k_{as,f5} \cdot \frac{\text{Clb5} \cdot \text{Cdc6}}{\text{mass}} + k_{pp,f6} \cdot \frac{\text{Cdc14} \cdot \text{F5P}}{\text{mass}} - (k_{di,f5} + V_{d,b5} + V_{kp,f6}) \cdot \text{F5} + k_g \cdot \text{F5}$$

$$\frac{\text{d F2P}}{\text{dt}} = V_{kp,f6} \cdot \text{F2} - (k_{pp,f6} \cdot \frac{\text{Cdc14}}{\text{mass}} + k_{d3,f6} + V_{d,b2}) \cdot \text{F2P} + k_g \cdot \text{F2P}$$

$$\frac{\text{d F5P}}{\text{dt}} = V_{kp,f6} \cdot \text{F5} - (k_{pp,f6} \cdot \frac{\text{Cdc14}}{\text{mass}} + k_{d3,f6} + V_{d,b5}) \cdot \text{F5P} + k_g \cdot \text{F5P}$$

$$\frac{\text{d Swi5T}}{\text{dt}} = k_{s,s5} \cdot \text{mSwi5} - k_{d,swi} \cdot \text{Swi5T} + k_g \cdot \text{Swi5T}$$

$$\frac{\text{d Swi5}}{\text{dt}} = k_{s,s5} \cdot \text{mSwi5} + k_{a,swi} \cdot \frac{\text{Cdc14}}{\text{mass}} \cdot (\text{Swi5T} - \text{Swi5}) - (k_{d,swi} + k_{i,swi} \cdot \frac{\text{Clb2}}{\text{mass}}) \cdot \text{Swi5} + k_g \cdot \text{Swi5}$$

$$\frac{\text{d APC\_P}}{\text{dt}} = k_{a,apc} \cdot \frac{\text{Clb2}}{\text{mass}} \cdot \frac{\text{APC} - \text{APC\_P}}{J_{a,apc} + \frac{\text{APC} - \text{APC\_P}}{c_{apc} \cdot \text{mass}}} - k_{i,apc} \cdot \frac{\text{APC\_P}}{J_{i,apc} + \frac{\text{APC\_P}}{c_{apc} \cdot \text{mass}}} + k_g \cdot \text{APC\_P}$$

Table 3.3: (Continued).

$$\frac{\text{d Cdc20T}}{\text{dt}} = k_{s,c20} \cdot \text{mCdc20} - k_{d,20} \cdot \text{Cdc20T} + k_g \cdot \text{Cdc20T}$$

$$\frac{\text{d Cdc20A}}{\text{dt}} = (k'_{a,20} + k''_{a,20} \cdot \frac{\text{APC\_P}}{\text{mass}}) \cdot (\text{Cdc20T} - \text{Cdc20A}) - (k_{mad2} + k_{d,20}) \cdot \text{Cdc20A} + k_g \cdot \text{Cdc20A}$$

$$\frac{\text{d Cdh1T}}{\text{dt}} = k_{s,cdh} \cdot \text{mass} \cdot \text{mCdh1} - k_{d,cdh} \cdot \text{Cdh1T} + k_g \cdot \text{Cdh1T}$$

$$\frac{\text{d Cdh1}}{\text{dt}} = k_{s,cdh} \cdot \text{mass} \cdot \text{mCdh1} - k_{d,cdh} \cdot \text{Cdh1} + V_{a,cdh} \cdot \frac{\text{Cdh1T} - \text{Cdh1}}{J_{a,cdh} + \frac{\text{Cdh1T} - \text{Cdh1}}{c_{cdh1} \cdot \text{mass}}} - V_{i,cdh} \cdot \frac{\text{Cdh1}}{J_{i,cdh} + \frac{\text{Cdh1}}{c_{cdh1} \cdot \text{mass}}} + k_g \cdot \text{Cdh1}$$

$$\frac{\text{d Tem1}}{\text{dt}} = k_{lte1} \cdot \frac{\text{Tem1T} - \text{Tem1}}{J_{a,tem} + \frac{\text{Tem1T} - \text{Tem1}}{c_{tem1} \cdot \text{mass}}} - k_{bub2} \cdot \frac{\text{Tem1}}{J_{i,tem} + \frac{\text{Tem1}}{c_{tem1} \cdot \text{mass}}} + k_g \cdot \text{Tem1}$$

$$\frac{\text{d Cdc15}}{\text{dt}} = (k'_{a,15} \cdot \frac{\text{Tem1T} - \text{Tem1}}{\text{mass}} + k''_{a,15} \cdot \frac{\text{Tem1}}{\text{mass}} + k'''_{a,15} \cdot \frac{\text{Cdc14}}{\text{mass}}) \cdot (\text{Cdc15T} - \text{Cdc15}) - k_{i,15} \cdot \text{Cdc15} + k_g \cdot \text{Cdc15}$$

$$\frac{\text{d Cdc14T}}{\text{dt}} = k_{s,14} \cdot \text{mass} \cdot \text{mCdc14} - k_{d,14} \cdot \text{Cdc14T} + k_g \cdot \text{Cdc14T}$$

$$\frac{\text{d Cdc14}}{\text{dt}} = k_{s,14} \cdot \text{mass} \cdot \text{mCdc14} - k_{d,14} \cdot \text{Cdc14} + k_{d,net} \cdot (\text{RENT} + \text{RENTP}) + k_{di,rent} \cdot \text{RENT} + k_{di,rentp} \cdot \text{RENTP} + k_g \cdot \text{Cdc14} - (k_{as,rent} \cdot \frac{\text{Net1}}{\text{mass}} + k_{as,rentp} \cdot \frac{\text{Net1P}}{\text{mass}}) \cdot \text{Cdc14}$$

$$\frac{\text{d Net1T}}{\text{dt}} = k_{s,net} \cdot \text{mass} \cdot \text{mNet1} - k_{d,net} \cdot \text{Net1T} + k_g \cdot \text{Net1T}$$

$$\frac{\text{d Net1}}{\text{dt}} = k_{s,net} \cdot \text{mass} \cdot \text{mNet1} - k_{d,net} \cdot \text{Net1} + k_{d,14} \cdot \text{RENT} + k_{di,rent} \cdot \text{RENT} - k_{as,rent} \cdot \frac{\text{Cdc14} \cdot \text{Net1}}{\text{mass}} + V_{pp,net} \cdot \text{Net1P} - V_{kp,net} \cdot \text{Net1} + k_g \cdot \text{Net1}$$

$$\frac{\text{d RENT}}{\text{dt}} = -(k_{d,14} + k_{d,net}) \cdot \text{RENT} - k_{di,rent} \cdot \text{RENT} + k_{as,rent} \cdot \frac{\text{Cdc14} \cdot \text{Net1}}{\text{mass}} + V_{pp,net} \cdot \text{RENTP} - V_{kp,net} \cdot \text{RENT} + k_g \cdot \text{RENT}$$

$$\frac{\text{d Pds1}}{\text{dt}} = k_{s,p1} \cdot \text{mPds1} + k_{di,esp} \cdot \text{PE} - (V_{d,pds} + k_{as,esp} \cdot \frac{\text{Esp1}}{\text{mass}}) \cdot \text{Pds1} + k_g \cdot \text{Pds1}$$

$$\frac{\text{d Esp1}}{\text{dt}} = -k_{as,esp} \cdot \frac{\text{Pds1} \cdot \text{Esp1}}{\text{mass}} + (k_{di,esp} + V_{d,pds}) \cdot \text{PE} + k_g \cdot \text{Esp1}$$

$$\frac{\text{d ORI}}{\text{dt}} = k_{s,ori} \cdot (e_{ori,b5} \cdot \text{Clb5} + e_{ori,b2} \cdot \text{Clb2}) - k_{d,ori} \cdot \text{ORI} + k_g \cdot \text{ORI}$$

$$\frac{\text{d BUD}}{\text{dt}} = k_{s,bud} \cdot (e_{bud,n2} \cdot \text{Cln2} + e_{bud,n3} \cdot \text{Cln3} + e_{bud,b5} \cdot \text{Clb5}) - k_{d,bud} \cdot \text{BUD} + k_g \cdot \text{BUD}$$

$$\frac{\text{d SPN}}{\text{dt}} = k_{s,spn} \cdot \frac{\text{Clb2}}{J_{spn} + \frac{\text{Clb2}}{c_{clb2} \cdot \text{mass}}} - k_{d,spn} \cdot \text{SPN} + k_g \cdot \text{SPN}$$

$$\frac{\text{d Tem1T}}{\text{dt}} = k_{s,tem1t} \cdot \text{mass} \cdot \text{mTem1} - k_{d,tem1t} \cdot \text{Tem1T} + k_g \cdot \text{Tem1T}$$

$$\frac{\text{d Cdc15T}}{\text{dt}} = k_{s,cdc15t} \cdot \text{mass} \cdot \text{mCdc15} - k_{d,cdc15t} \cdot \text{Cdc15T} + k_g \cdot \text{Cdc15T}$$

$$\frac{\text{d Esp1T}}{\text{dt}} = k_{s,esp1t} \cdot \text{mass} \cdot \text{mEsp1} - k_{d,esp1t} \cdot \text{Esp1T} + k_g \cdot \text{Esp1T}$$

$$\frac{\text{d SBFT}}{\text{dt}} = k_{s,sbft} \cdot \text{mass} \cdot \text{mSBF} - k_{d,sbft} \cdot \text{SBFT} + k_g \cdot \text{SBFT}$$

$$\frac{\text{d MBFT}}{\text{dt}} = k_{s,mbft} \cdot \text{mass} \cdot \text{mMBF} - k_{d,mbft} \cdot \text{MBFT} + k_g \cdot \text{MBFT}$$

$$\frac{\text{d Mcm1T}}{\text{dt}} = k_{s,mcm1t} \cdot \text{mass} \cdot \text{mMcm1} - k_{d,mcm1t} \cdot \text{Mcm1T} + k_g \cdot \text{Mcm1T}$$

$$\frac{\text{d APC}}{\text{dt}} = k_{s,apct} \cdot \text{mass} \cdot \text{mAPC} - k_{d,apct} \cdot \text{APC} + k_g \cdot \text{APC}$$

$$\text{Cln3} = \frac{C_0 \cdot D_{n3} \cdot \text{mass}^2}{J_{n3} + D_{n3} \cdot \text{mass}}$$

$$\text{Bck2} = B_0 \cdot \text{mass}^2$$

$$\text{Sic1T} = \text{Sic1} + \text{Sic1P} + \text{C2} + \text{C2P} + \text{C5} + \text{C5P}$$

$$\text{Cdc6T} = \text{Cdc6} + \text{Cdc6P} + \text{F2} + \text{F2P} + \text{F5} + \text{F5P}$$

$$\text{RENTP} = \text{Cdc14T} - \text{RENT} - \text{Cdc14}$$

$$\text{Net1P} = \text{Net1T} - \text{Net1} - \text{Cdc14T} + \text{Cdc14}$$

Table 3.3: (Continued).

$$
\begin{aligned}
\text{PE} =& \text{Esp1T} - \text{Esp1} \\
\text{SBF} =& G(V_{a,sbf}, V_{i,sbf}, J_{a,sbf}, J_{i,sbf}) \cdot \text{SBFT} \\
\text{MBF} =& G(V_{a,sbf}, V_{i,sbf}, J_{a,sbf}, J_{i,sbf}) \cdot \text{MBFT} \\
\text{Mcm1} =& G(k_{a,mcm} \cdot \frac{\text{Clb2}}{\text{mass}}, k_{i,mcm}, J_{a,mcm}, J_{i,mcm}) \cdot \text{Mcm1T} \\
V_{a,sbf} =& k_{a,sbf}(e_{sbf,n2} \cdot [\text{Cln2}] + e_{sbf,n3}([\text{Cln3}] + [\text{Bck2}]) + e_{sbf,b5} \cdot [\text{Clb5}]) \\
V_{i,sbf} =& k'_{i,sbf} + k''_{i,sbf} \cdot [\text{Clb2}] \\
V_{d,b5} =& k'_{d,b5} + k''_{d,b5} \cdot [\text{Cdc20A}] \\
V_{d,b2} =& k'_{d,b2} + k''_{d,b2} \cdot [\text{Cdh1}] + k_{d,b2p} \cdot [\text{Cdc20A}] \\
V_{kp,c1} =& k_{d1,c1} + \frac{k_{d2,c1}}{J_{d2,c1} + [\text{Sic1T}]}(e_{c1,n3} \cdot [\text{Cln3}] + e_{c1,k2} \cdot [\text{Bck2}] + e_{c1,n2} \cdot [\text{Cln2}] + e_{c1,b5} \cdot [\text{Clb5}] + e_{c1,b2} \cdot [\text{Clb2}]) \\
V_{kp,f6} =& k_{d1,f6} + \frac{k_{d2,f6}}{J_{d2,f6} + [\text{Cdc6T}]}(e_{f6,n3} \cdot [\text{Cln3}] + e_{f6,k2} \cdot [\text{Bck2}] + e_{f6,n2} \cdot [\text{Cln2}] + e_{f6,b5} \cdot [\text{Clb5}] + e_{f6,b2} \cdot [\text{Clb2}]) \\
V_{a,cdh} =& k'_{a,cdh} + k''_{a,cdh} \cdot [\text{Cdc14}] \\
V_{i,cdh} =& k'_{i,cdh} + k''_{i,cdh}(e_{cdh,n3} \cdot [\text{Cln3}] + e_{cdh,n2} \cdot [\text{Cln2}] + e_{cdh,b2} \cdot [\text{Clb2}] + e_{cdh,b5} \cdot [\text{Clb5}]) \\
V_{pp,net} =& k'_{pp,net} + k''_{pp,net} \cdot [\text{Cdc55}] \\
V_{kp,net} =& (k'_{kp,net} + k''_{kp,net} \cdot [\text{Cdc15}]) \cdot \text{mass} \\
V_{d,ppx} =& k'_{d,ppx} + k''_{d,ppx}(J_{20,ppx} + [\text{Cdc20A}]) \cdot \frac{J_{pds}}{J_{pds} + [\text{Pds1}]} \\
V_{d,pds} =& k'_{d1,pds} + k''_{d2,pds} \cdot [\text{Cdc20A}] + k''_{d3,pds} \cdot [\text{Cdh1}]
\end{aligned}
$$

At the end, the synthesis and degradation of mRNAs are added by SSA. Reactions related to mRNAs are illustrated in section 3.3. The details of the implementation, mechanism, and accuracy and efficiency analysis of the hybrid model were discussed in [37]. [37] showed that the results of the hybrid model match very well with experimental statistics for budding yeast cells, and the simulations of hybrid run much faster than the simulations of SSA. It only takes the hybrid method (Fortran program) 400 seconds to simulate $5,500$ cell cycles, while for SSA (Fortran program) it takes a few days to execute the same task.

Chapter 4

Visualization Tool for Budding Yeast Cell Cycle Models

4.1 Motivation

If the results of the mathematical model match well with wet-lab experimental data, we have more confidence that our understanding of the control mechanism is correct. Otherwise, further study is needed. In order to validate a mathematical model, it is necessary to compare the computed behaviors of the model with the corresponding observed phenotypes of the cells, including wild types and mutant cases. For the cell cycle model, we are interested in whether the mutant is viable or inviable (i.e. fail to proliferate), as well as the populations of species for each event. If viable, what is the mass of the cell at each checkpoint of the cell cycle? What is the duration of each phase? If inviable, at what phase does it stop? All of the features are hard to see intuitively from the numerical results of the mathematical models unless for very well trained eyes. Biologists observe the cells through a microscope, however, the output of the mathematical model is a set of data.

Table 4.1 is the output of Chen's model [7] for wild-type daughter cell in glucose, which contains 40 columns including time, mass and 38 species, and 2188 rows of discrete time until 500 minutes. Obviously, it will be a boring, tired and time-consuming job to compare this data with the experimental results. Thus data visualization is needed here. Data visualization creates and studies the visual representation of data in a pictorial or graphical format. It is a powerful means to visualize large amounts of complex data that could not communicate when presented as text in spreadsheets or tables, and thus make human brain to process information easier and quicker. It is not only a useful method for our budding yeast cell visualization in this thesis but also an important research field of computer science. From the beginning of recorded time until 2003, our society created 5 billion gigabytes (exabytes) of data. In 2011, the same amount was made every two days. In 2013, the same amount of data

Table 4.1: The output of Chen's model for wild-type daughter cell in glucose.

time	mass	BUD	ORI	SPN	Cln2	Clb2	Clb5	Cdh1	Cdc14	Cdc20	...
0.0000	1.2060	0.0009	0.0085	0.0306	0.0653	0.1469	0.0518	0.9305	0.4683	0.4443	...
0.0019	1.2060	0.0013	0.0085	0.0307	0.0652	0.1464	0.0517	0.9309	0.4681	0.4442	...
0.0039	1.2061	0.0018	0.0085	0.0308	0.0652	0.1459	0.0516	0.9313	0.4679	0.4442	...
0.0058	1.2061	0.0022	0.0086	0.0308	0.0652	0.1454	0.0515	0.9318	0.4677	0.4441	...
0.0143	1.2062	0.0041	0.0087	0.0313	0.0652	0.1432	0.0511	0.9336	0.4667	0.4438	...
0.0228	1.2062	0.0059	0.0088	0.0317	0.0651	0.1409	0.0506	0.9354	0.4656	0.4435	...
0.0312	1.2063	0.0078	0.0089	0.0321	0.0650	0.1387	0.0502	0.9372	0.4646	0.4432	...
0.0397	1.2064	0.0096	0.0090	0.0325	0.0650	0.1365	0.0497	0.9390	0.4636	0.4429	...
0.0627	1.2066	0.0144	0.0093	0.0336	0.0648	0.1306	0.0485	0.9437	0.4610	0.4421	...
0.0857	1.2068	0.0190	0.0096	0.0346	0.0647	0.1248	0.0473	0.9482	0.4583	0.4413	...
0.1087	1.2070	0.0234	0.0099	0.0356	0.0645	0.1191	0.0461	0.9526	0.4557	0.4404	...
0.1318	1.2072	0.0277	0.0102	0.0366	0.0644	0.1135	0.0448	0.9568	0.4531	0.4395	...
0.1623	1.2075	0.0330	0.0106	0.0379	0.0642	0.1064	0.0432	0.9620	0.4497	0.4384	...
0.1928	1.2078	0.0381	0.0109	0.0391	0.0640	0.0995	0.0415	0.9669	0.4463	0.4371	...
0.2233	1.2081	0.0429	0.0113	0.0403	0.0638	0.0928	0.0398	0.9714	0.4431	0.4359	...
0.2538	1.2084	0.0475	0.0116	0.0414	0.0636	0.0865	0.0381	0.9755	0.4399	0.4346	...
0.2844	1.2087	0.0517	0.0119	0.0425	0.0634	0.0805	0.0364	0.9792	0.4368	0.4333	...
0.3409	1.2092	0.0589	0.0125	0.0443	0.0631	0.0701	0.0333	0.9848	0.4312	0.4308	...
0.3975	1.2097	0.0652	0.0130	0.0459	0.0627	0.0607	0.0301	0.9892	0.4260	0.4282	...
0.4541	1.2102	0.0708	0.0135	0.0474	0.0624	0.0524	0.0270	0.9923	0.4210	0.4255	...
0.5107	1.2108	0.0756	0.0140	0.0487	0.0621	0.0452	0.0240	0.9944	0.4163	0.4228	...
0.5672	1.2113	0.0798	0.0144	0.0498	0.0619	0.0388	0.0211	0.9958	0.4118	0.4199	...
0.6308	1.2119	0.0837	0.0148	0.0509	0.0616	0.0328	0.0180	0.9969	0.4071	0.4166	...
0.6944	1.2125	0.0870	0.0152	0.0519	0.0614	0.0277	0.0152	0.9976	0.4027	0.4132	...
0.7579	1.2131	0.0898	0.0156	0.0527	0.0612	0.0235	0.0126	0.9980	0.3986	0.4097	...
0.8215	1.2137	0.0920	0.0159	0.0533	0.0610	0.0200	0.0103	0.9984	0.3948	0.4061	...
0.8851	1.2143	0.0937	0.0162	0.0538	0.0608	0.0172	0.0084	0.9986	0.3912	0.4024	...
0.9487	1.2149	0.0952	0.0165	0.0543	0.0607	0.0149	0.0067	0.9988	0.3878	0.3987	...
1.0147	1.2155	0.0963	0.0167	0.0547	0.0607	0.0129	0.0054	0.9989	0.3846	0.3948	...
1.0807	1.2161	0.0972	0.0170	0.0550	0.0606	0.0112	0.0042	0.9991	0.3816	0.3908	...
1.1467	1.2167	0.0979	0.0172	0.0552	0.0607	0.0099	0.0034	0.9992	0.3788	0.3868	...
⋮	⋮	⋮	⋮	⋮	⋮	⋮	⋮	⋮	⋮	⋮	⋮

was created in every 10 minutes. 90% of the data in nowaday's world were created in the last two years alone [18]. Data visualization makes data more accessible such that we can visually and comprehensively obtain the useful information. Most of the famous technical companies, for instance, Google, Facebook, and Amazon, make their critical business decisions by using data visualization.

Chen et al. compared the computed results of the mathematical model with experimental observations by plotting the data on a line chart, which is used to identify patterns between sets of data. Figure 4.1 is the corresponding line chart of data in Table 4.1. These trajectories of oscillations of all these properties indicate that the cell is viable. We can get near-accurate estimates of the important properties from the line chart, for example, the length of G_1 phase is around 36 minutes, the cycle time is around 101 minutes, the mass at division is around 2.61, and the relative concentrations of proteins, and so on. However, Figure 4.1 only can be read by a person with deep knowledge in the cell cycle control mechanism. A successful visualization may present complicated information in a way that can be quickly and easily understood by specialists and non-specialists alike. In addition, although Figure 4.1 provides some useful information, the overall graphic of the cell is still not visible and users have to

try to form a mental model of the cell cycle. Moreover, every adjustment of time range (time axis) and species (values on the y axis) is implemented by changing the code. So we design our visualization tool, which combines static, dynamic, and interactive elements, where the proliferation of budding yeast cell is simulated as dynamical animation. With the help of this visualization tool, we can easily and intuitively see many key steps in the budding yeast cell cycle procedure, such as bud emergence, DNA synthesis, mitosis, cell division, and the current populations of species. It is essentially a powerful web-based interface, with simple menus and several selection buttons, to guide users to create visualizations of the simulation results, where users can select the mutant type, the mathematical model, the simulation time, proteins to be displayed, and so on, to visualize the behavior of the cell cycle.

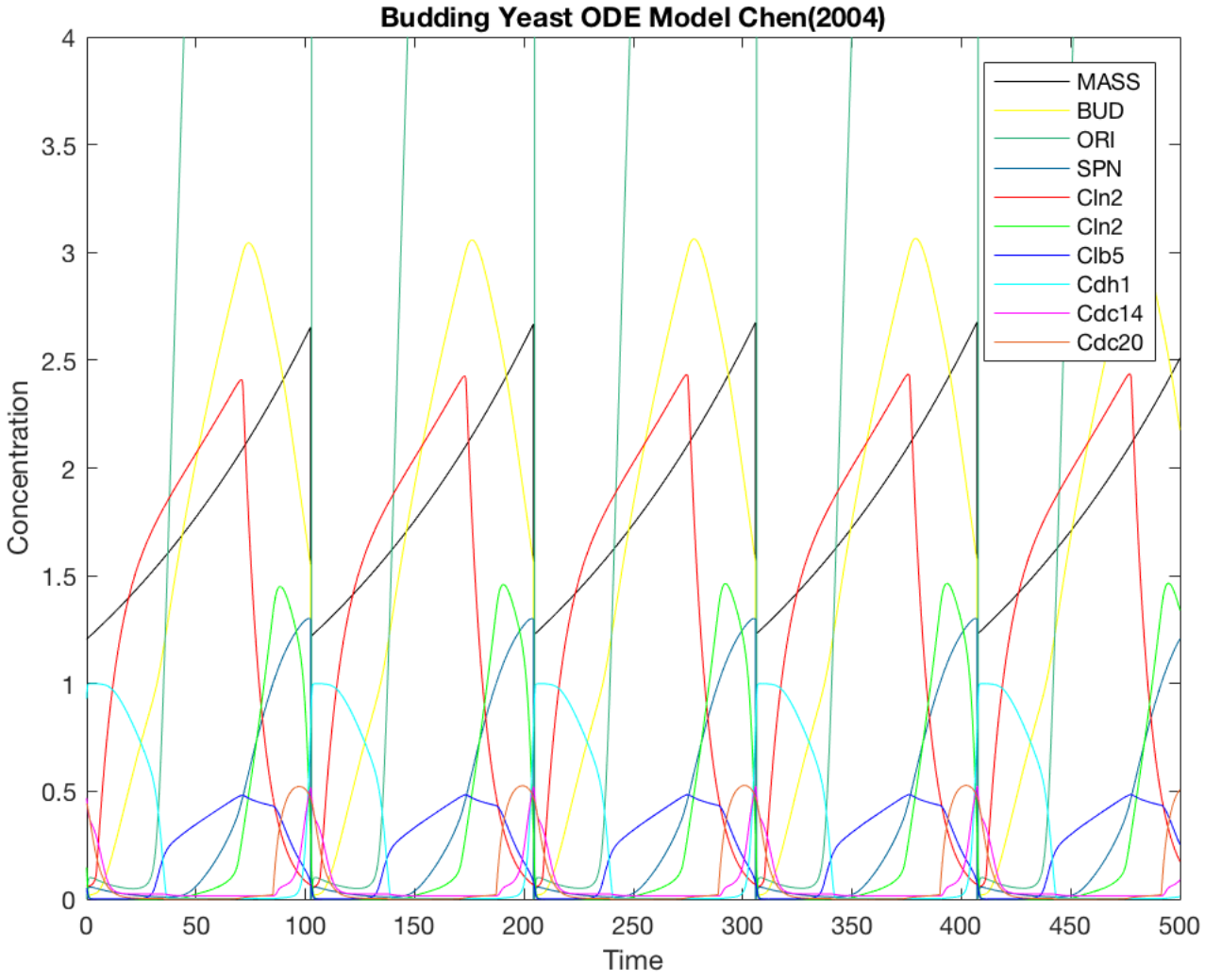

Figure 4.1: Simulation of the data from Chen's Model for wild-type daughter cell in glucose.

4.2 Toolkit and Interface

Our visualization of budding yeast cell cycle is mainly generated by D3 (Data-Driven Documents) and jQuery. D3 is a JavaScript library for loading data into a web page and creating the visualization from that data. jQuery is also a JavaScript library which makes DOM (Document Object Model) element selection, animation, events handling, and AJAX (Asynchronous JavaScript And XML) much easier and simpler. We choose the web-based technology and publish the visualization on the web: `http://people.cs.vt.edu/~ycao/yeast_cell_visualization/visualization.html`, so that anyone using an up to data web browser can visit it. It is the quickest way to get feedback from the general public, as well as experimental biologists, and to encourage us to improve models of the molecular mechanism of the budding yeast cell cycle.

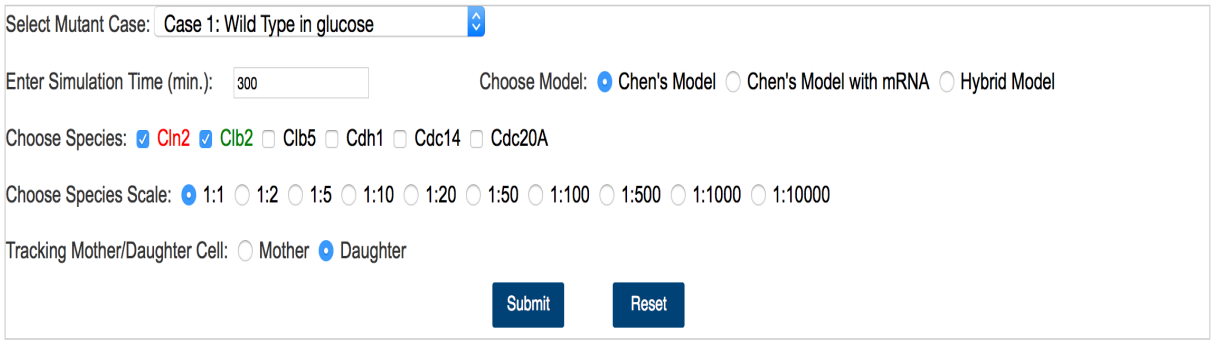

Figure 4.2: Interface.

Figure 4.2 illustrates the web-based interface which guides users to visualize the budding yeast cell cycle simulation results. The "Selection Mutant Case" is a drop-down list contains all mutant cases that will be discussed in this thesis, which can display once the user clicks the arrow at the right side (Figure 4.3). The case number refers to the mutant case number in Table 3.1. By default, the wild-type in glucose is selected when the page is loaded. From results of cells with $CLB2$-$db\Delta$ $clb5\Delta$ mutant in [37], we know the range of the budding yeast cell cycle times is from 0 to 500 minutes. For the mathematical model, the cell is considered as inviable if its cycle time is longer than 500 minutes. So we only visualize the cell cycle up to 500 minutes. Users can enter any real number between 0 to 500 in the text area after "Enter Simulation Time" to help our visualization tool to choose the time duration of the visualization. The three mathematical model selections in the control panel have been discussed in Chapter 3. But it is necessary to notice that the Chen's Model and the Chen's Model with mRNA here are the transferred population versions. The species are the proteins introduced in section 2.2. A single or multiple species can be selected by the user and changed to the specific color automatically. For inviable cells, the populations of some species will grow to a huge number, so scaling the populations can prevent species get very clustered in the animated cell. For example, the scale $1:10$ indicates that the number

of species will appear in the cell is given by the real population divided by 10. Tracking mother (or daughter) means the daughter (or mother) cell will be thrown away after each division. Once the *submit* button is clicked, a line chart of the selected species and given time range will display on the web page, immediately, coupled with a time slider to play the animation of the budding yeast cell cycle.

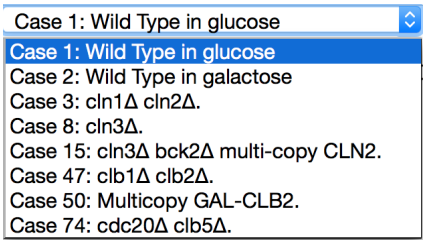

Figure 4.3: Selected mutant cases.

4.3 Interactive Line Chart

In our visualization, we will still use the line chart to show the populations of species against the time. The line chart is a basic and easy form of visualization and is successful to provide the trend and the near-accurate estimate of the data. It is helpful to investigate the reactions or relationships of species. Our line chart supports interactions that users can control the displayed species and time range, and hover over the line chart to see the accurate values of each point. Figure 4.4 is the created line chart of the species and the simulation time in Figure 4.7.

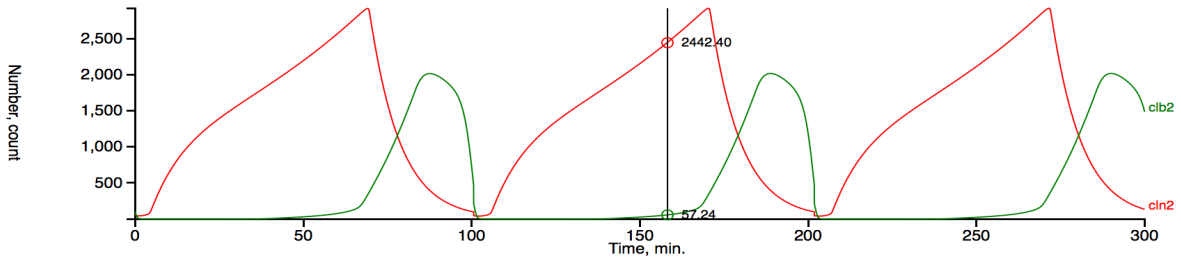

Figure 4.4: Interactive Multi-line Chart.

4.4 Animation

Animation visualization is more visually engaging than static visualizations such as the line chart introduced above, especially for time-varying data. Figure 4.10 illustrates the simulated cell when it stops at the end of one cell cycle, the yellow area represents cell, the blue area represents nucleus, the two small black points are the spindle poles, the purple curves represent chromosomes in the nucleus, and the black straight lines connecting the poles and chromosomes are spindles, obviously. The red and green tiny points are the selected and scaled species which appear in the cell randomly. Users can play or drag the slider to view the animation. Texts after "Time" and "Mass" show the precise values of the current time and mass.

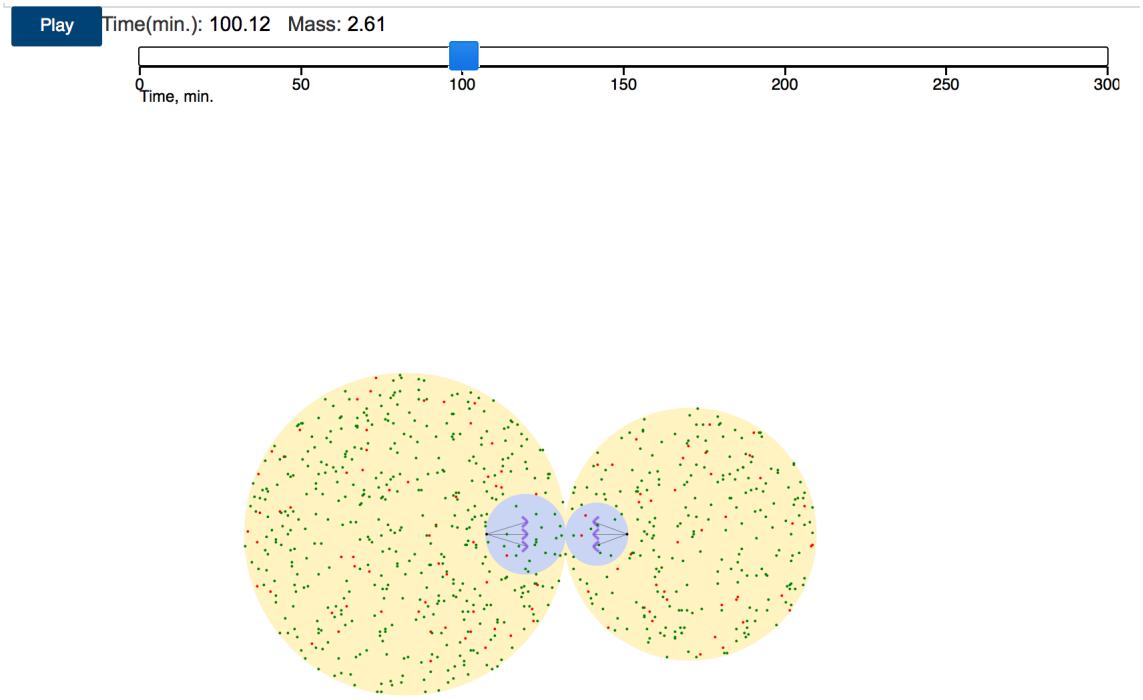

Figure 4.5: Animation of the cell division.

4.4.1 Flags of Events

In the visualization of the budding yeast cell cycle, there are three major checkpoints: bud emergence, start DNA synthesis, and chromosome alignment on spindle completed. In Chen's model, three event flag variables [BUD], [ORI], and [SPN] were used to link the output of the mathematical model to these events. Except them, the values of mass and [Esp1] are equally important. All flags of the events are listed in Table 4.2. During one cell cycle, the mass of

the cell keeps increasing. However, the cell will lose the ability to divide or proliferate if its mass becomes greater than 10, and the corresponding simulation is considered as inviable. In Table 4.2, [ ] represents the concentration. We can use the formulas in Table 4.3 to transform populations into concentrations, where the constant $CN = 0.602 \cdot 30/1.206$.

Table 4.2: Flags of events.

Flags	**Events**
mass decreases	start new cell cycle
[BUD] = 1	bud emergence
[ORI] = 1	start DNA synthesis
[SPN] = 1	chromosome alignment on spindle completed
[Esp1] = 0.1	start sister chromatids separation
mass = 10	cell loses the ability to proliferate

There are total three orders for the occurrence of bud emergence, DNA synthesis, and chromosome alignment.

(i) bud emergence→DNA synthesis→chromosome alignment, i.e.

$$[\text{BUD}] = 1 \rightarrow [\text{ORI}] = 1 \rightarrow [\text{SPN}] = 1. \tag{4.4.1}$$

Normally, wild-type cells always follow this order.

(ii) DNA synthesis→bud emergence→chromosome alignment, i.e.

$$[\text{ORI}] = 1 \rightarrow [\text{BUD}] = 1 \rightarrow [\text{SPN}] = 1. \tag{4.4.2}$$

For some mutants (the cells can be either viable or inviable), bud emerges after DNA synthesis.

(iii) DNA synthesis→chromosome alignment→bud emergence, i.e.

$$[\text{ORI}] = 1 \rightarrow [\text{SPN}] = 1 \rightarrow [\text{BUD}] = 1. \tag{4.4.3}$$

This case only takes place in some mutants (the cells are normally inviable). The spindle poles move randomly in the nucleus and the separated chromosomes do not go to the bud. Mostly, cells lose abilities to divide or proliferate.

Notation: The DNA synthesis must happen before chromosomes alignment.

Table 4.3: Transformation from population into concentration.

Population	**Concentration**
BUD	[BUD] = BUD/(10·mass·CN)
ORI	[ORI] = ORI/(10·mass·CN)
SPN	[SPN] = SPN/(10·mass·CN)
Esp1	[Esp1] = Esp1/(33·mass·CN)

4.4.2 Functions to Design the Animation

We define all checkpoints in our visualization and their corresponding times in Table 4.4. The subscripts $o, b, r, m, c, p, n, s, e$ are integers, and represent the indexes of the discrete time.

Table 4.4: Checkpoints of the visualization and their corresponding times.

Time	**Events**
t_o	Start new cell cycle.
t_b	Bud Emergence ([BUD]=1).
t_r	Start DNA synthesis. Spindle pole duplicates and becomes visible ([ORI]=1).
t_m	The duplicated pole starts to move to the daughter nucleus.
t_c	Chromosomes condensed and become visible.
t_p	Spindles emerge and start to pull the chromosomes.
t_n	The duplicated pole reaches the nucleus envelop.
t_s	Alignment of all chromosomes on the metaphase plate ([SPN]=1).
t_e	End of one cell cycle.

(1) Growth rate of the cell

Let $V(t)$ = the given mass of the cell at time t, $V_m(t)$ = the mass of the mother cell at time t, and $V_b(t)$ = the mass of the bud at time t. Then $V(t) = V_m(t) + V_b(t)$. It is obvious that $V_m(t_j) = V(t_j), V_b(t_j) = 0$ for $o \leq j < b$. After bud emergence, the increment of mass is $\Delta V_j = V(t_j) - V(t_{j-1}), b \leq j \leq e$. The masses of the mother cell and the bud are

$$V_m(t_j) = V_m(t_{j-1}) + \Delta V_j \cdot \frac{V_b(t_{j-1})}{V_m(t_{j-1}) + V_b(t_{j-1})}, \quad b \leq j \leq e,$$

$$V_b(t_j) = V_b(t_{j-1}) + \Delta V_j \cdot \frac{V_m(t_{j-1})}{V_m(t_{j-1}) + V_b(t_{j-1})}, \quad b \leq j \leq e.$$

(2) Position of the bud

In our visualization, the position of the mother cell is fixed, however, the position of the bud has to change since it emerges. Assume the center of the mother cell is (x_1, y_1), x_1 and

y_1 are given constants. The center of the bud is $(x_2(t), y_2)$, where $x_2(t)$ depends on the time and $y_2 = y_1$ is constant. The radii of the mother cell and the bud are $R_1(t) = 10 \cdot (V_m(t))^{1/3}$ and $R_2(t) = 10 \cdot (V_b(t))^{1/3}$, respectively. For the cell whose chromosomes will be aligned on the metaphase plate, the position of the bud at $t = t_s$ is important. So we define $x_2(t)$ as a piecewise function.

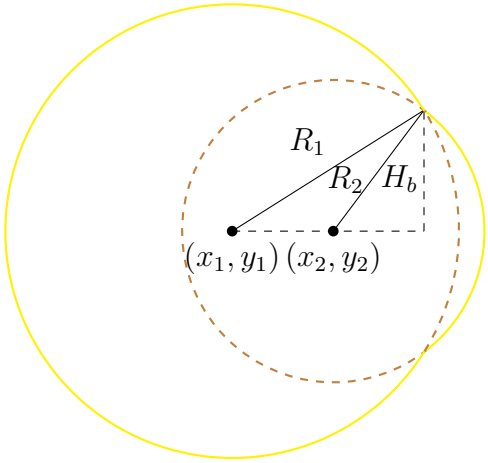

Figure 4.6: The cell at $t = t_b$.

Figure 4.6 shows the cell at bud emergence, with $H_b = \frac{4}{5}R_2(t_b)$. Then

$$x_2(t_b) = x_1 + \sqrt{R_1^2(t_b) - H_b^2} - \sqrt{R_2^2(t_b) - H_b^2}.$$

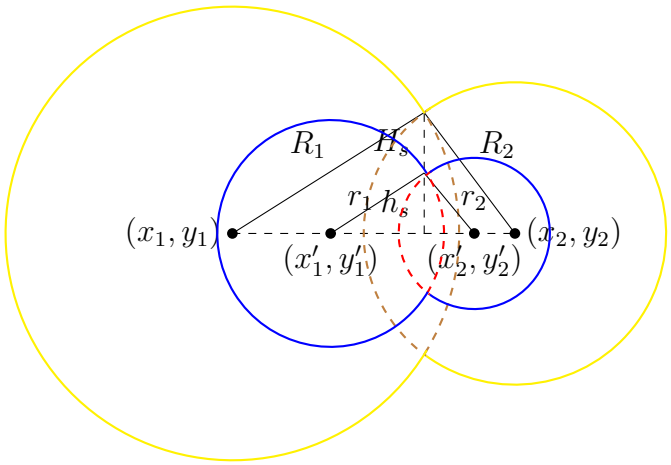

Figure 4.7: The cell with nucleus at $t = t_s$.

Figure 4.7 illustrates the cell when chromosomes aligned, with $H_s = \frac{4}{5}R_2(t_s)$. Then

$$x_2(t_s) = x_1 + \sqrt{R_1^2(t_s) - H_s^2} + \sqrt{R_2^2(t_s) - H_s^2}.$$

If the cell is viable, the bud will be isolated from the mother cell at $t = t_e$. Then $x_2(t_e) = x_1 + R_1(t_e) + R_2(t_e)$. Therefore,

$$x_2(t) = \begin{cases} x_2(t_b) + (j-b)\dfrac{x_2(t_s) - x_2(t_b)}{s-b}, & t = t_j, \quad b \le j \le s, \\ x_2(t_s) + (j-s)\dfrac{x_2(t_e) - x_2(t_s)}{e-s}, & t = t_j, \quad s < j \le e. \end{cases} \tag{4.4.4}$$

(3) Position of the nucleus

In a viable cell cycle, the nucleus will move forward to the bud. Let the centers of the mother nucleus and the daughter nucleus be $(x_1'(t), y_1')$ and $(x_2'(t), y_2')$, respectively, where both of $x_1'(t)$ and $x_2'(t)$ depend on the time. y_1' and y_2' are constants satisfying $y_1' = y_2' = y_1 = y_2$. We assume that the daughter nucleus appears at the same time of bud emergence. The radius of the mother nucleus is $r_1(t) = R_1(t)/4$, and $r_2(t) = R_2(t)/4$ is the radius of the daughter nucleus.

Imagine Figure 4.6 as the graph of the nucleus. $x_1'(t_b) = x_1$, and

$$x_2'(t_b) = x_1 + \sqrt{r_1^2(t_b) - h_b^2} - \sqrt{r_2^2(t_b) - h_b^2},$$

where $h_b = \frac{4}{5}r_2(t_b)$. From Figure 4.7, we have

$$\begin{aligned} x_1'(t_s) &= x_1 + \sqrt{R_1^2(t_s) - H_s^2} - \sqrt{r_1^2(t_s) - h_s^2}, \\ x_2'(t_s) &= x_1 + \sqrt{R_1^2(t_s) - H_s^2} + \sqrt{r_2^2(t_s) - h_s^2}, \end{aligned}$$

where $h_s = \frac{4}{5}r_2(t_s)$. It is easy to get that $x_1'(t_e) = x_1 + R_1(t_e) - r_1(t_e)$ and $x_2'(t_e) = x_1 + R_1(t_e) + r_2(t_e)$. Then

$$x_1'(t) = \begin{cases} x_1, & t = t_j, \quad o \le j \le b, \\ x_1 + (j-b)\dfrac{x_1'(t_s) - x_1'(t_b)}{s-b}, & t = t_j, \quad b < j \le s, \\ x_1'(t_s) + (j-s)\dfrac{x_1'(t_e) - x_1'(t_s)}{e-s}, & t = t_j, \quad s < j \le e, \end{cases} \tag{4.4.5}$$

and

$$x_2'(t) = \begin{cases} x_2'(t_b) + (j-b)\dfrac{x_2'(t_s) - x_2'(t_b)}{s-b}, & t = t_j, \quad b \le j \le s, \\ x_2'(t_s) + (j-s)\dfrac{x_2'(t_e) - x_2'(t_s)}{e-s}, & t = t_j, \quad s < j \le e. \end{cases} \tag{4.4.6}$$

(4) Positions of chromosomes

In our visualization, there are three chromosomes. In a real cell, the sizes of the chromosomes never change throughout the whole cell cycle. So we need to define the half height or width (d in Figure 4.8) of the condensed chromosomes, such that the chromosomes always stay inside the nucleus. Figure 4.8 illustrates the positions of the chromosomes when they emerge in the mother nucleus and get aligned at $t = t_s$. In Figure 4.8, the blue circle is the mother nucleus at $t = t_c$, and the area bounded by the dashed red arcs is same as the corresponding area in Figure 4.7. b_1, b_2 and b_3 are constants during a cell cycle, and a_1, a_2 and a_3 are variables depend on time t.

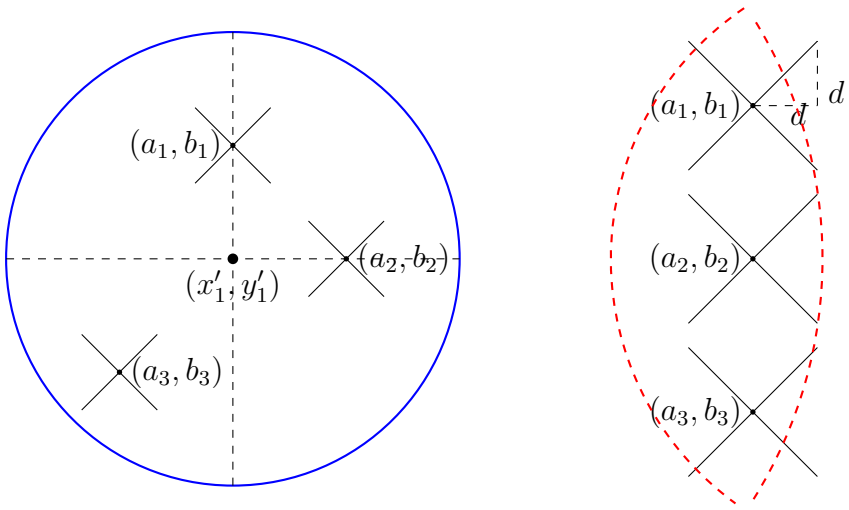

Figure 4.8: Positions of the chromosomes at $t = t_c$ and $t = t_s$ for orders (4.4.1) and (4.4.2).

We pick h as the smaller one of $r_1(t_c)$ and h_s, and define $d = \frac{8}{15}h$, $b_1 = y_1' + d + \frac{1}{10}h$, $b_2 = y_1'$ and $b_3 = y_1' - d - \frac{1}{10}h$. Then,

$$\begin{cases} a_1(t) = x_1'(t), & t = t_j, \quad c \le j \le p, \\ a_2(t) = x_1'(t) + r_1(t)/2, & t = t_j, \quad c \le j \le p, \\ a_3(t) = x_1'(t) - r_1(t)/2, & t = t_j, \quad c \le j \le p, \\ a_1(t) = a_1(t_p) + (j-p)\dfrac{a_1(t_s) - a_1(t_p)}{s-p}, & t = t_j, \quad p < j \le s, \\ a_2(t) = a_2(t_p) + (j-p)\dfrac{a_2(t_s) - a_2(t_p)}{s-p}, & t = t_j, \quad p < j \le s, \\ a_2(t) = a_2(t_p) + (j-p)\dfrac{a_2(t_s) - a_2(t_p)}{s-p}, & t = t_j, \quad p < j \le s, \end{cases} \tag{4.4.7}$$

where $a_1(t_s) = a_2(t_s) = a_3(t_s) = x_1 + \sqrt{R_1^2(t_s) - H_s^2}$.

(5) Positions of spindle poles

Let $(x_1''(t), y_1)$ and $(x_2''(t), y_1)$ represent the positions of poles. The mother pole always attaches the envelope of the mother nucleus. Thus, $x_1''(t) = x_1'(t) - r_1(t) + r_p,\ t = t_j,\ r \leq j \leq e$, where the constant r_p is the radius of the pole. Let $x_2''(t_m) = x_1''(t_m) + \frac{1}{10} r_1(t_m)$. Referring to Figure 4.7, $x_2''(t_n) = x_1'(t_n) + \sqrt{r_1^2(t_n) - h_n^2} + \sqrt{r_2^2(t_n) - h_n^2} + r_2(t_n) - r_p$, with $h_n = \frac{4}{5} r_2(t_n)$. Then,

$$\begin{cases} x_2''(t) = x_2''(t_m) + (j-m)\dfrac{x_2''(t_n) - x_2''(t_m)}{n-m}, & t = t_j, \quad m \leq j \leq n, \\ x_2''(t) = x_2'(t) + r_2(t) - r_p, & t = t_j, \quad n < j \leq e. \end{cases} \tag{4.4.8}$$

4.4.3 Process

Based on the functions built by (4.4.4) - (4.4.8), it is easy to implement the visualizations of cases (4.4.1)-(4.4.3). Figures 4.9-4.11 illustrate the processes of the visualizations in detail.

All pictures in Figure 4.9 are the screenshots of the visualization for the wild-type cell in glucose. The cell follows the order of (4.4.1). t_o, t_b, t_r, t_s and t_e can be determined uniquely from the Flags (Table 4.2) if they exist, otherwise, for example, the [SPN] never goes to 1 or the cell is inviable, we set the non-exist time to a hug number. There are no specific Flags that can help us to find the time t_c, t_m and t_n, because these events happen quickly and overlap sometimes. So we divide the duration from t_r to t_s evenly, and define $t_c = t_r + t_{\lfloor (s-r)/4 \rfloor},\ t_m = t_r + t_{\lfloor (s-r)/2 \rfloor}$ and $t_n = t_r + t_{\lfloor 3\cdot(s-r)/4 \rfloor}$.

All pictures in Figure 4.10 are the screenshots of the visualization for $cln1\Delta$ $cln2\Delta$ mutant. The cell follows the order of (4.4.2). Similarly, we define $t_c = t_r + t_{\lfloor (b-r)/2 \rfloor},\ t_m = t_b + t_{\lfloor (s-b)/3 \rfloor},\ t_n = t_b + t_{\lfloor 2\cdot(s-r)/3 \rfloor}$.

All pictures in Figure 4.10 are the screenshots of the visualization for multi-copy $GAL\text{-}CLB2$ mutant, except the last one. Multi-copy $GAL\text{-}CLB2$ mutant is inviabe and never divides. We will discuss this mutant case in Chapter 5. We define $t_c = t_m = t_r + t_{\lfloor (s-r)/3 \rfloor}, t_n = t_r + t_{\lfloor 2\cdot(s-b)/3 \rfloor}$. The design of the visualization here is kind of different from the previous two cases. It is not necessary to use the functions in section 4.4.2 to find the metaphase plate, because the chromosomes aligned in the middle of the mother nucleus. We will not set up new functions to find the positions of chromosomes, nucleus or poles. All of them are expected to be very simple to find.

(I) $t = t_o$
Start new cell cycle.

(II) $t = t_b$
Bud emerges and nucleus starts to move to the bud.

(III) $t = t_r = t_m$
Duplicated Spindle poles emerge.

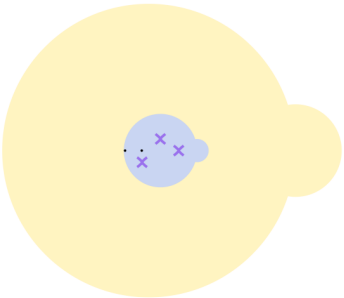

(IV) $t = t_c$
Chromosomes condensed.

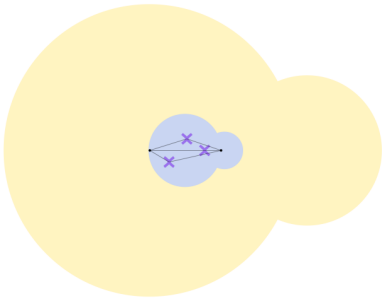

(V) $t = t_p$
Spindles emerge and start to pull the chromosomes.

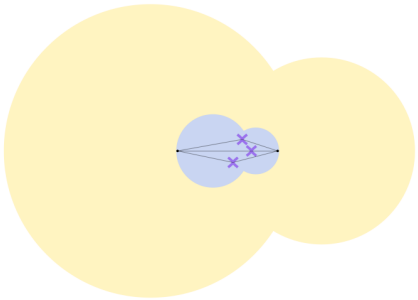

(VI) $t = t_n$
Pole of daughter nucleus at its end position.

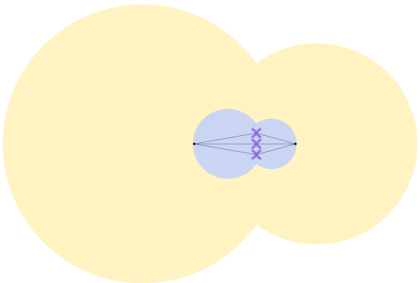

(VII) $t = t_s$
Alignment of all chromosomes on the metaphase plate.

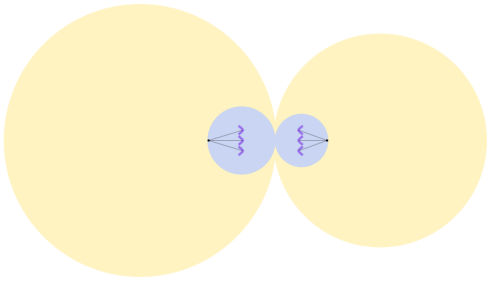

(VIII) $t = t_e$
Cell divides.

Figure 4.9: Checkpoints for visualization of order (4.4.1).

(I) $t = t_o$
Start new cell cycle.

(II) $t = t_r$
Poles of spindles emergence.

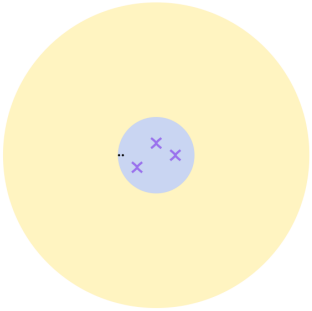

(III) $t = t_c$
Chromosomes condensation finished.

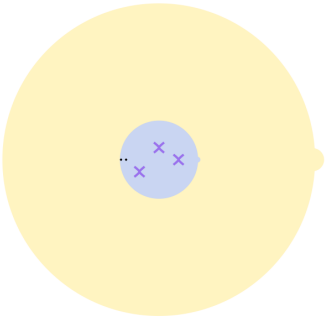

(IV) $t = t_b = t_m$
Bud emerges and nucleus starts to move to the bud.

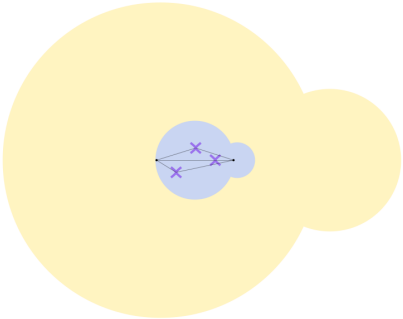

(V) $t = t_p$
Spindles emerge and start to pull the chromosomes.

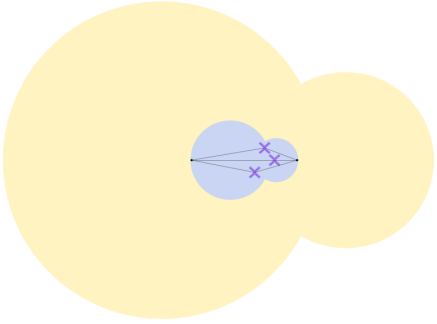

(VI) $t = t_n$
Pole of bud nucleus moved to the right end point.

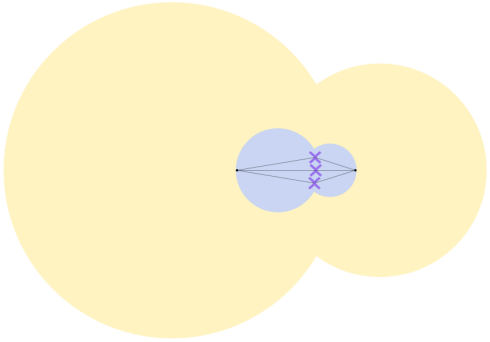

(VII) $t = t_s$
Alignment of all chromosomes on the metaphase plate.

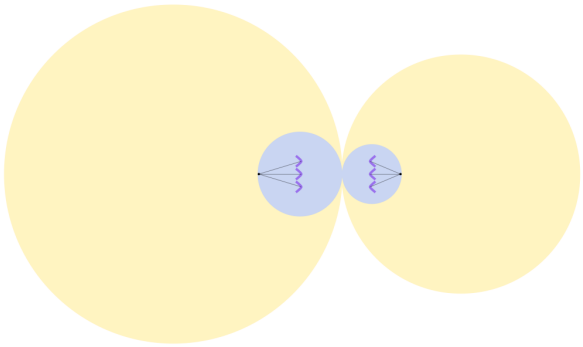

(VIII) $t = t_e$
Cell divides.

Figure 4.10: Checkpoints for visualization of order (4.4.2).

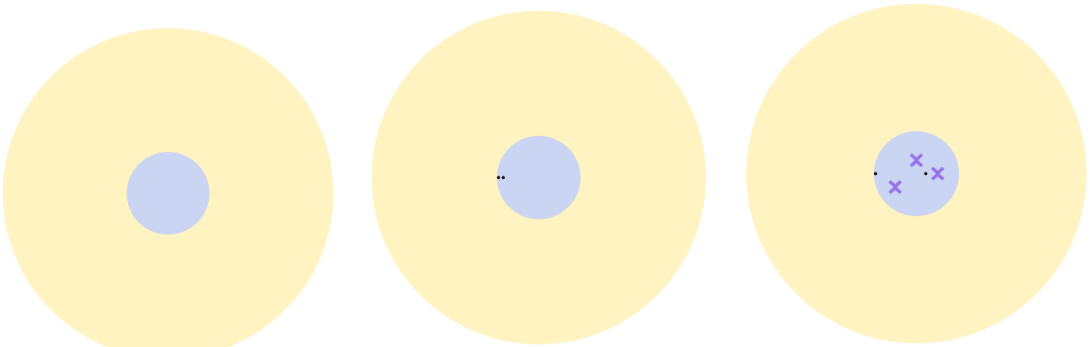

(I) $t = t_o$
Start new cell cycle.

(II) $t = t_r = t_m$
Poles of spindles emergence.

(III) $t = t_c$
Chromosomes condensation finished.

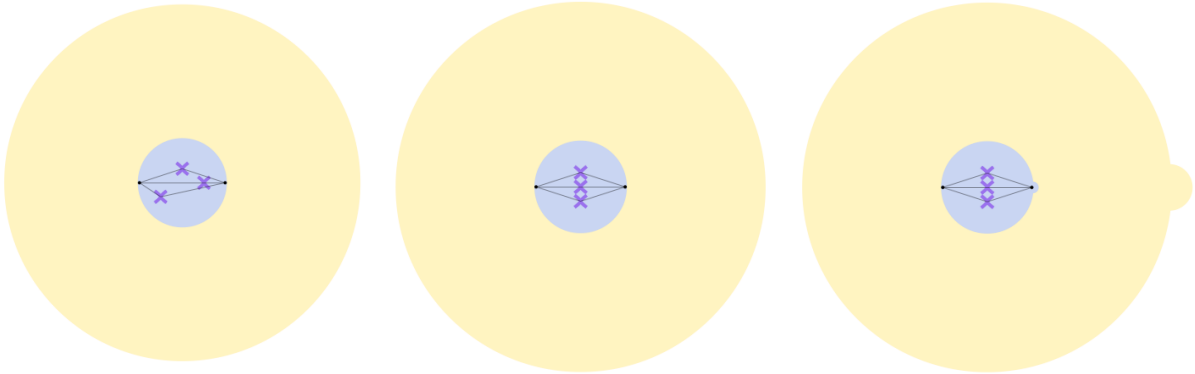

(IV) $t = t_p = t_n$
Spindles emerge and start to pull the chromosomes.

(V) $t = t_s$
Alignment of all chromosomes.

(VII) $t = t_b$
Bud emerges and nucleus starts to move to the bud.

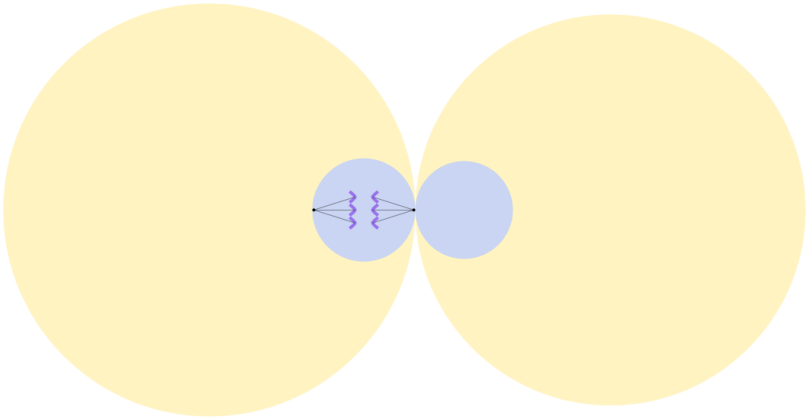

(VIII) $t = t_e$
Cell divides.

Figure 4.11: Checkpoints for visualization of order (4.4.3).

Chapter 5

Results

In this chapter, we use some typical mutant cases to demonstrate our visualization tool.

5.1 Viable Cases Study

We compare the visualizations and experimental observations for four kinds of viable cells, including wild-types in glucose and galactose, mutant $cln1\Delta$ $cln2\Delta$, and mutant $cln3\Delta$, in Table 5.1, where the visualization results contain all simulations of the three mathematical models. For wide type (WT) in glucose, the visualization shows that the cell proliferation always follows the process of Figure 4.9 in deterministic models, however, sometimes DNA synthesis happens before bud emergence in the hybrid model, due to the effect of noise, and demonstrates the special feature of the hybrid model. $cln1\Delta$ $cln2\Delta$ is a viable mutant whose procedure of cell cycle is described in Figure 4.10, where DNA synthesis happens before bud emergence. Mutant $cln3\Delta$ is viable and follows the most regular order of "bud emergence $\rightarrow$ DNA synthesis $\rightarrow$ chromosomes alignment". Table 5.1 demonstrates that our visualization for the viable cell is successful.

Table 5.1: Comparisons between visualizations and experiments for No.1, 2, 3, 8 in Table 3.1.

	WT in glucose	WT in galactose	$cln1\Delta$ $cln2\Delta$	$cln3\Delta$
Change of parameters			ksn2"=0	Dn3=0
Experimental result	Viable	Viable	Viable	Viable
Visualization result	Viable	Viable	Viable	Viable
Process	Figures 4.9&4.10	Figure 4.9	Figure 4.10	Figure 4.9

From the visualization we can easily, visually and intuitively observe the important features of the cell cycle, including the mass at each checkpoint, the duration of each phase,

and the populations of species for each event. Figure 5.1 is an example to illustrate it. All graphs in Figure 5.1 come from the Chen's model with tracking daughter cell. The displayed protein in the cell is Cln2, which is related to bud emergence. The line chart below the cell in the visualization shows us the population and its pattern of Cln2 during the time duration. The time of bud emergence can be obtained from the value of "Time" or the position of the slider. The precise mass of the cell is the value after "Mass", meanwhile, it can be seen from the size of the cell.

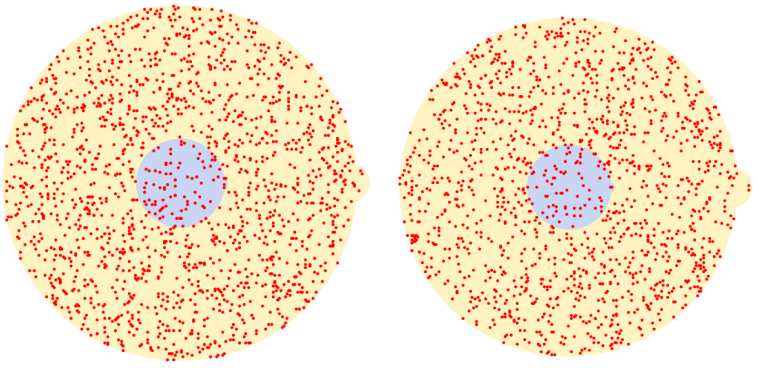

(I) WT in glucose
Time ≈ 32 min., Mass ≈ 1.5,
Population of Cln2 ≈ 2000.

(II) WT in galactose
Time ≈ 34 min., Mass ≈ 1.4,
Population of Cln2 ≈ 1400.

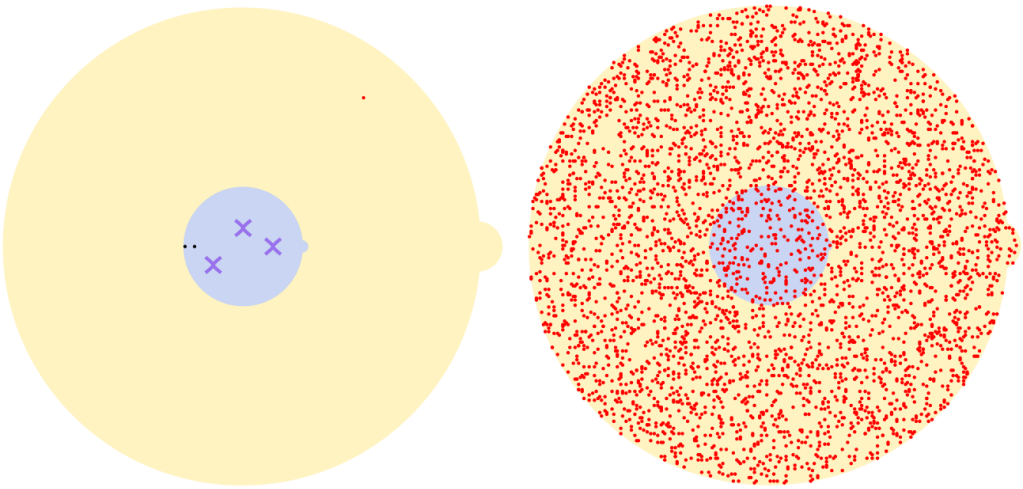

(III) *cln*1Δ *cln*2Δ
Time ≈ 110 min., Mass ≈ 2.8,
Population of Cln2 ≈ 1.

(IV) *cln*3Δ
Time ≈ 96 min., Mass ≈ 2.5,
Population of Cln2 ≈ 5000.

Figure 5.1: Comparisons of two wild-types, mutant *cln*1Δ *cln*2Δ, and mutant *cln*3Δ at bud emergence.

It is straightforward to compare the visualized cell with the observed phenotype to check

the molecular mechanism and its mathematical model. Figure 5.1 proves another advantage of our visualization that is visual comparisons of different kinds of mutant cells. From Figure 5.1 we can see, at the onset of bud emergence, mutant cells have bigger size and longer duration than wild-type cells. All (I), (II) and (III) follow order (4.4.1), but mutant case needs more Cln2 to bud than wild-types.

5.2 Inviable Cases Study

We discussed the four typical viable cells. Figure 4.5 is the moment of the cell divides into two daughter cells, which shows that the simulated cell is viable. If inviable, the cell never arrives this step, it loses the ability to divide and stops at some time before it. Next, we discuss some inviable mutant cases. Our visualization can easily demonstrate at which phase the cell arrests.

1. *cln*3Δ *bck*2Δ multi-copy $CLN2$. It is the No.15 mutant case in Table 3.1. Change of parameters: B0=0, Dn3=0, ksn2"=1.5 (=10 copies). Experimental result: Inviable, G_1 arrest. Because high copy CLN2 containing plasmid can not rescue the lethality of *cln*3Δ *bck*2Δ [39].

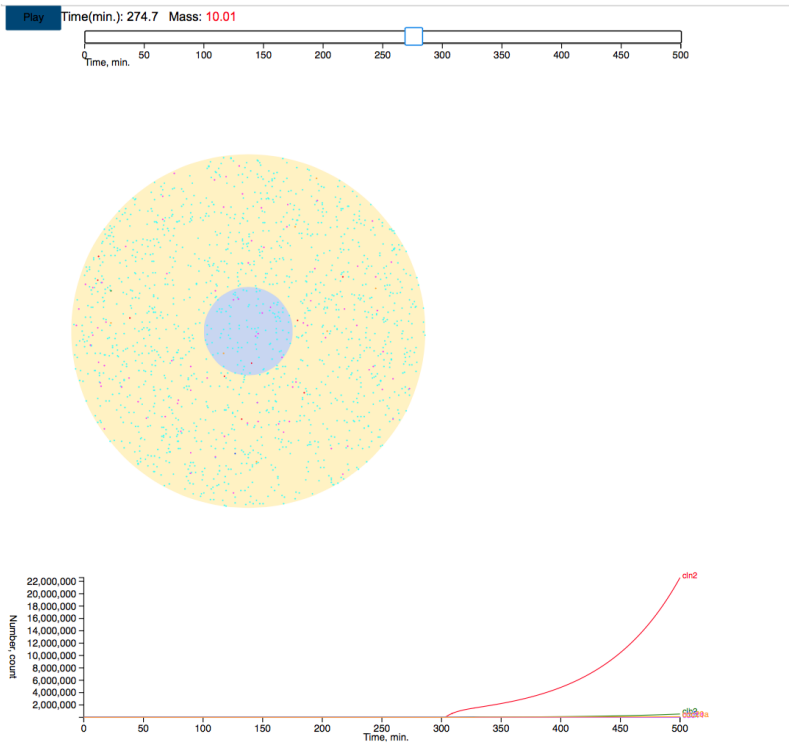

Figure 5.2: Visualization of the *cln*3Δ *bck*2Δ multi-copy $CLN2$ mutant for Chen's Model tracking daughter cell. The selected species scale is 1:10.

Figure 5.2 illustrates the moment where the cell arrests. We think G_1 phase as the period from the beginning of a new cell cycle to the start of DNA synthesis. So this mutant case is inviable and G_1 arrest. The population of Cln2 is increasing for the whole time duration. Our simulation results totally match the experimental behaviors. It is necessary to point out that the first cell cycle is viable and the others are inviable and stop at G_1 phase for the hybrid model.

2. *clb*1Δ *clb*2Δ. It is No.47 in Table 3.1. Change of parameters: ksb2'=ksb2"=0. Experimental result: Inviable, G_2 arrest [31].

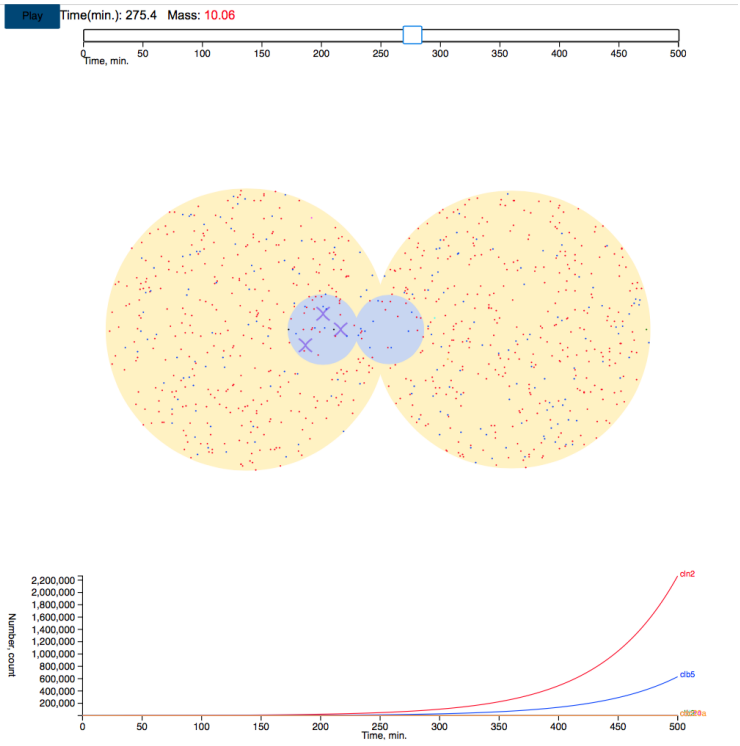

Figure 5.3: Visualization of the *clb*1Δ *clb*2Δ mutant for Chen's model tracking daughter cell. The selected species scale is 1:100.

Figure 5.3 is the visualization of mutant No. 47. Similar with No. 15, the cell arrests because of its mass greater than 10. As discussed in section 4.4.1, there are three primary Flags for the design of the visualization. However, there is not a specific Flag to label the end time of the S phase. It is even harder to determine the right start or end time of the S phase from experiment, because DNA synthesis is not visible and there is an overlap of phases. Usually the S phase takes about 30 minutes for the budding yeast cell cycle. So for simulated inviable mutant cases, the S phase arrest has never been checked. In our visualization, we roughly define the period from chromosomes condensation to chromosomes alignment (i.e. [SPN]=1) as the G_2 phase. The simulated cell in Figure 5.3 is G_2 arrest, which matches with

the corresponding experimental result.

3. *cdc*20Δ *clb*5Δ. It is No.74 in Table 3.1. Change of parameters: ks20'=ks20"=0, ksb5'=ksb5"=0. Experimental result: Inviable, Metaphase arrest.

We discussed G_1 and G_2 phases arrest. Now we study the cases of the M phase arrest. During the M phase, we mainly focus on the Metaphase and Telophase. If the cell arrests at the time of [SPN]=1, i.e., all chromosomes get aligned on the metaphase plate and the sister chromatids never separate, we say the cell is at Metaphase arrest. Otherwise, if the sister chromatids separate but the cell never divides, we say the cell arrests at Telophase. The experimental result shows that *cdc*20Δ *clb*5Δ mutant is Metaphase arrest, however, our visualization (Figure 5.4) is Telophase arrest. This result is acceptable for Chen's model, as there is any flag in Chen's model to denote the separation of sister chromatids, and the time from Metaphase to Telophase is really short, and both of them belong to the M phase.

It is observed that Esp1 is needed for sister chromatids separation. We tried to introduce one non-given Flag, i.e. [Esp1]=0.1, as a trigger of sister chromatids separation, to our visualization system, where 0.1 comes from experimental data. Unfortunately, it only works for partial cell cycles. So we will continue to define different event flags that can distinguish the Metaphase and the Telophse to improve our visualization tool in the future.

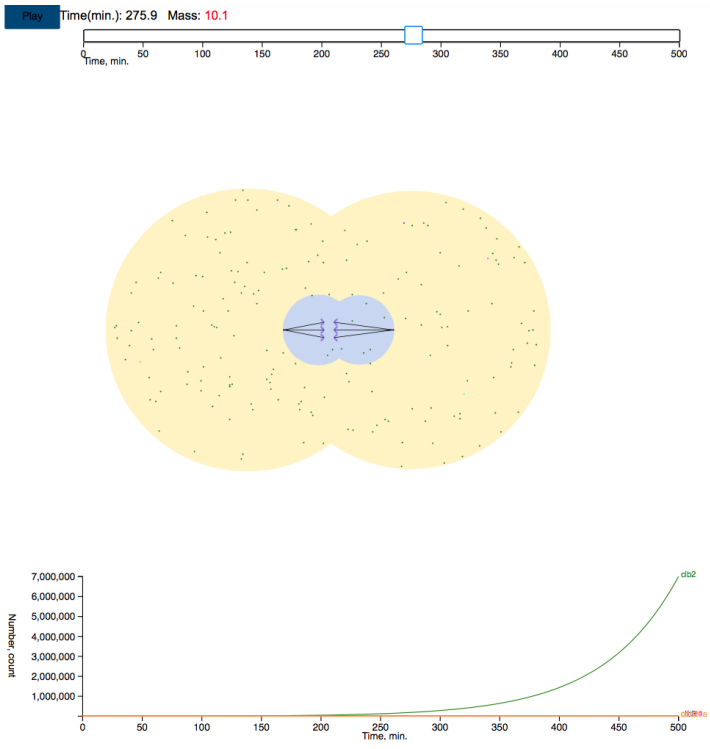

Figure 5.4: Visualization of the *cdc*20Δ *clb*5Δ mutant for Chen's Model tracking daughter cell. The selected species scale is 1:1000.

4: Multi-copy *GAL-CLB2*. It is No. 50 in Table 3.1. Change of parameters: ksb2'=0.8, MDT=150. Experimental result: Inviable, Telophase arrest.

The animated cell arrests at Telophase (Figure 5.5), which matches with the experimental result. So our work is successful for this case as well.

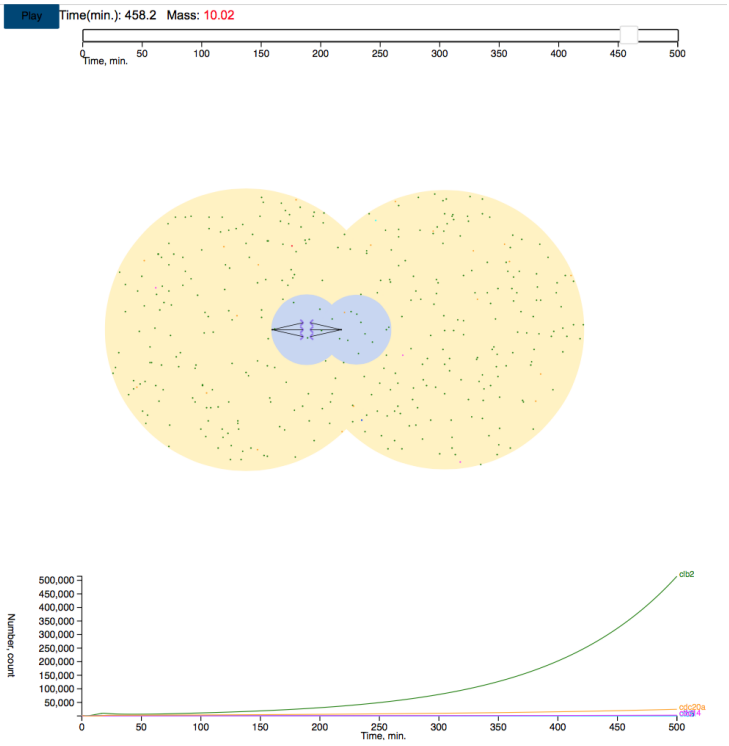

Figure 5.5: Visualization of the Multi-copy *GAL-CLB2* mutant for Chen's model tracking daughter cell. The selected species scale is 1:1000.

Chapter 6

Conclusion and Future Work

Many mathematical models have been proposed to simulate the control mechanism (at the molecular level) of the regulatory budding yeast cell cycle. We build a visualization tool to help users to visualize the simulation results of these mathematical models. By comparing the visualization of wild-type cells and certain interesting viable and inviable mutant cells to the wet-lab experimental observations, we have shown that our tool successfully creates the visualization of the budding yeast cell cycle model. The visualization tool shows great advantages over traditional line charts. One advantage is that it is more likely to find the needed information through our interactive and animated visualization. Another advantage is that it allows users without any biological background to make sense of the cell cycle process. Our visualization tool has been successfully applied to visualize all viable mutants and inviable mutants arrest at G_1, G_2 and M phases. However, we cannot distinguish Metaphase and Telophase so far. In the near future, we will improve the model and focus on the control mechanism of the budding yeast cell cycles to unveil another Flag which triggers the sister chromatids separation. Meanwhile, we plan to import many simulation results of other mutant cases into the visualization tool. In the long future, we expect this visualization tool to become a useful silicon experiment tool for biological modeling studies.

Bibliography

[1] Alexandru, G., Zachariae, W., Schleiffer, A. and Nasmyth, K. (1999). Sister chromatid separation and chromosome re-duplication are regulated by different mechanisms in response to spindle damage. EMBO J. 18:2707-2721.

[2] Amon, A., Irniger, S. and Nasmyth, K. (1994). Closing the cell cycle circle in yeast: G2 cyclin proteolysis initiated at mitosis persists until the activation of G1 cyclins in the next cycle. Cell 77:1037-1050.

[3] Ball, D. A., Ahn,T.-H., Wang, P., Chen, K. C., Cao, Y., Tyson, J. J., Peccoud, J., and Baumann, W. T. (2011). Stochastic exit from mitosis in budding yeast. Cell Cycle, 10(6):9991009.

[4] Bardin, A. and Amon, A. (2001). Men and sin: what's the difference? Nat. Rev. Mol. Cell Biol. 2:815-826.

[5] Baumer, M., Braus, G.H. and Irniger, S. (2000). Two different models of cyclin Clb2 proteolysis during mitosis in Saccharomyces cerevisiae. FEBS Lett 468:142-148.

[6] Chen, K.C., Csikasz-Nagy, A., Gyorffy, B., Val, J., Novak, B. and Tyson, J.J. (2000). Kinetic analysis of a molecular model of the budding yeast cell cycle. *Mol. Biol. Cell* 11:369-391.

[7] Chen, K.C., Calzone, L., Csikasz-Nagy, A., Cross, F.R., Novak, B. and Tyson, J.J. (2004). Integrative analysis of cell cycle control in budding yeast. *Mol. Biol. Cell* 15:3841-3862.

[8] Ciosk, R., Zachariae, W., Michaelis, C., Shevchenko, A., Mann, M. and Nasmyth, K. (1998). An ESP1/PDS1 complex regulates loss of sister chromatid cohesion at the metaphase to anaphase transition in yeast. Cell 93:1067-1076.

[9] Dirick, L., Bohm, T. and Nasmyth, K. (1995). Roles and regulation of Cln/Cdc28 kinases at the start of the cell cycle of Saccharomyces cerevisiae. EMBO J. 14:4803-4813.

[10] Elsasser, S., Chi, Y., Yang, P. and Campbell, J.L. (1999). Phosphorylation controls timing of Cdc6p destruction: a biochemical analysis. Mol. Biol. Cell 10:3263-3267.

[11] Gillespie, D. T. (1976). A general method for numerically simulating the stochastic time evo-lution of coupled chemical reactions. Journal of Computational Physics, 22(4):403-434.

[12] Gillespie, D. T. (1977). Exact stochastic simulation of coupled chemical reactions. Journal of Physical Chemistry, 81(25):2340-2361.

[13] Irniger, S., Piatti, S., Michaelis, C. and Nasmyth, K. (1995). Genes involved in sister chromatid separation are needed for B-type cyclin proteolysis in budding yeast. Cell 81:269-278.

[14] Irniger, S. and Nasmyth, K. (1997). The anaphase-promoting complex is required in G1 arrested yeast cells to inhibit B-type cyclin accumulation and to prevent uncontrolled entry into S-phase. J. Cell Sci. 110:1523-1531.

[15] Jaspersen, S.L., Charles, J.F. and Morgan, D.O. (1999). Inhibitory phosphorylation of the APC regulator Hct1 is controlled by the kinase Cdc28 and the phosphatase Cdc14. Curr. Biol. 11:227-236.

[16] Lim, H.H., Goh, P.-Y. and Surana, U. (1998). Cdc20 is essential for the cyclosome-mediated proteolysis of both Pds1 and Clb2 during M phase in budding yeast. Curr. Biol. 8:231-234.

[17] Liu, Z., Pu, Y., Li, Fi. Shaffer, C. A., Hoops, S., Tyson, J. J., and Cao, Y. (2012). Hybrid modeling and simulation of stochastic effects on progression through the eukaryotic cell cycle. Journal of Chemical Physics, 136(3).

[18] Liu, Y. (2014). Big data and predictive business analytics. The Journal of Business Forecasting, 33, 40-42.

[19] Mitchison, J.M. (1971). The Biology of the Cell Cycle, Cambridge, United Kingdom: Cambridge University Press.

[20] Murray, Andrew Wood & Hunt, Tim, 1943-1993, The cell cycle : an introduction, W.H. Freeman, New York.

[21] Nasmyth, K., Peters, J.-M. and Uhlmann, F. (2000). Splitting the chromosome: cutting the ties that bind sister chromatids. Science 288:1379-1384.

[22] Pedraza, J. M. and Paulsson, J. (2008). Effects of molecular memory and bursting on uctuations in gene expression. Science, 319:339343.

[23] Prinz, S., Hwang, E.S., Visintin, R. and Amon, A. (1998). The regulation of Cdc20 proteolysis reveals a role for the APC components Cdc23 and Cdc27 during S phase and early mitosis. Curr. Biol. 8:750-760.

[24] Schwob, E. and Nasmyth, K.(1993). CLB5 and CLB6, a new pair of B cyclins involved in DNA replication in Saccharomyces cerevisiae. Genes Dev. 7:1160-1175.

[25] Schwob, E., Bohm, T., Mendenhall, M.D. and Nasmyth, K. (1994). The B-type cyclin kinase inhibitor p40sic1 controls the G1 to S transition in S. cerevisiae. Cell 79:233-244.

[26] Seufert, W., Futcher, B. and Jentsch, S. (1995). Role of a ubiquitin-conjugating enzyme in degradation of S- and M-phase cyclins. Nature 373:78-81.

[27] Shirayama, M., Zachariae, W., Ciosk, R. and Nasmyth, K. (1998). The Polo-like kinase Cdc5p and the WD-repeat protein Cdc20p/fizzy are regulators and substrates of the anaphase promoting complex in Saccharomyces cerevisiae. EMBO J. 17:1336-1349.

[28] Shirayama, M., Toth, A., Galova, M. and Nasmyth, K. (1999). APC(CDC20) promotes exit from mitosis by destroying the anaphase inhibitor Pds1 and cyclin Clb5. Nature 402:203-207.

[29] Spellman, P.T., Sherlock, G., Zhang, M.Q., Iyer, V.R., Anders, K., Eisen, M.B., Brown, P.O., Botstein, D. and Futcher, B. (1998). Comprehensive identification of cell cycle-regulated genes of the yeast Saccharomyces cerevisiae by microarray hybridization. Mol. Biol. Cell 9:3273-3297.

[30] Stuart, D. and Wittenberg, C. (1995). CLN3, not positive feedback, determines the timing of CLN2 transcription in cycling cells. Genes Dev. 9:2780-2794.

[31] Surana, U., Robitsch, H., Price, C., Schuster, T., Fitch, I., Futcher, A.B. and Nasmyth, K. (1991). The role of CDC28 and cyclins during mitosis in the budding yeast S. cerevisiae. Cell 65:145-161.

[32] Thornton, B.R. and Toczyski, D.P. (2003). Securin and B-cyclin/CDK are the only essential targets of the APC. Nat. Cell Biol. 5:1090-1094.

[33] Tinker-Kulberg, R.L. and Morgan, D.O. (1999). Pds1 and Esp1 control both anaphase and mitotic exit in normal cells and after DNA damage. Genes Dev. 13:1936-1949.

[34] Tyers, M., Tokiwa, G. and Futcher B. (1993). Comparison of the Saccharomyces cerevisiae G1 cyclins: Cln3 may be an upstream activator of Cln1, Cln2 and other cyclins. EMBO J. 12:1955-68.

[35] Visintin, R., Prinz, S. and Amon, A. (1997). CDC20 and CDH1: a family of substrate-specific activators of APC-dependent proteolysis. Science 278:460-463.

[36] Visintin, R., Craig, K., Hwang, E.S., Prinz, S., Tyers, M. and Amon, A. (1998). The phosphatase Cdc14 triggers mitotic exit by reversal of Cdk-dependent phosphorylation. Mol. Cell 2:709-718.

[37] Wang, S., Ahmadian, M., Chen, M., Tyson, J.J., Cao, Y (2016). A Hybrid Stochastic Model of the Budding Yeast Cell Cycle Control Mechanism.

[38] Wasch, R. and Cross, F. (2002). APC-dependent proteolysis of the mitotic cyclin Clb2 is essential for mitotic exit. Nature 418:556-562.

[39] Wijnen, H., and Futcher, B. (1999) Genetic analysis of the shared role of CLN3 and BCK2 at the G1-S transition in Saccharomyces cerevisiae. Genetics 153:1131-1143.

[40] Wittenberg, C., Sugimoto, K. and Reed, S I. (1990). G1-specific cyclins of S. cerevisiae: cell cycle periodicity, regulation by mating pheromone, and association with p34CDC28 protein kinase. Cell 62:225-237.

[41] Yamamoto, A., Guacci, V. and Koshland, D. (1996). Pds1p, an inhibitor of anaphase in budding yeast, plays a critical role in the APC and checkpoint pathway(s). J. Cell Biol. 133:99-110.

[42] Yanagida, M. (2000). Cell cycle mechanisms of sister chromatid separation; roles of Cut1/separin and Cut2/securin. Genes Cells 5:1-8.

[43] Yeong, F.M., Lim, H.H., Padmashree, C.G. and Surana, U. (2000). Exit of mitosis in budding yeast: biphasic inactivation of the Cdc28-Clb2 mitotic kinase and the role of Cdc20. Mol. Cell 5:501-511.

[44] Zachariae, W., Schwab, M., Nasmyth, K. and Seufert, W. (1998). Control of cyclin ubiquitination by CDK-regulated binding of Hct1 to the anaphase promoting complex. Science 282:1721-1724.

[45] Zachariae, W. (1999). Progress into and out of mitosis. Curr. Opin. Cell Biol. 11:708-716.